Bioorganic Chemistry 91 (2019) 103155

Contents lists available at ScienceDirect

Bioorganic Chemistry

journal homepage: www.elsevier.com/locate/bioorg

Synthesis of 3-indolylmethyl substituted (pyrazolo/benzo)triazinone derivatives under Pd/Cu-catalysis: Identification of potent inhibitors of chorismate mutase (CM)

Gangireddy Sujeevan Reddy[a,b], Ampalam Venkata Snehalatha[a], Rebecca Kristina Edwin[a], Kazi Amirul Hossain[a], Varadaraj Bhat Giliyaru[b], Raghu Chandrashekhar Hariharapura[b], G. Gautham Shenoy[b], Parimal Misra[a], Manojit Pal[a,*]

[a] Dr Reddy's Institute of Life Sciences, University of Hyderabad Campus, Gachibowli, Hyderabad 500 046, India
[b] Manipal College of Pharmaceutical Sciences, Manipal Academy of Higher Education, Madhav Nagar, Manipal 576 104, Karnataka, India

ARTICLE INFO

Keywords:
Triazinone
Indole
Pyrazole
Palladium
Chorismate mutase

ABSTRACT

The chorismate mutase (CM) is considered as an attractive target for the identification of potential antitubercular agents due to its absence in animals but not in bacteria. A series of 3-indolylmethyl substituted pyrazolotriazinone derivatives were designed and docked into CM *in silico* as potential inhibitors. These compounds were efficiently synthesized using the Pd/Cu-catalyzed coupling-cyclization in a single pot involving the construction of indole ring. The methodology was later extended to the preparation of corresponding benzo analogs of pyrazolotriazinones i.e. 3-indolylmethyl substituted benzotriazinone derivatives. Several of these novel compounds showed significant inhibition of CM when tested *in vitro* at 30 μM. The SAR (Structure-Activity-Relationship) studies suggested that benzotriazinone moiety was more favorable over the pyrazolotriazinone ring. The two best active compounds showed IC_{50} ~ 0.4–0.9 μM (better than the reference/known compounds used) and no toxicity till 30 μM *in vitro*.

1. Introduction

Tuberculosis or TB is a common and infectious lung disease generally caused by the bacteria called *Mycobacterium tuberculosis* (MTB) [1]. Roughly, 25% of the world population is assumed to be infected by TB [2]. Indeed, TB remained one of the leading causes of death worldwide due to (i) the extended duration (6–9 months) of treatment, (ii) higher prevalence of (multi or extensive) drug resistance, (iii) co-morbidity with HIV-AIDS and (iv) decreased interest/effort in anti-infective drug research. The chorismate mutase or CM (EC 5.4.99.5) that catalyzes the Claisen rearrangement of chorismate to prephenate is considered as an attractive target for the identification of effective antibacterial agents due to its absence in animals but not in bacteria [3–5]. While several inhibitors of CM have been reported earlier [3] the potent inhibitors possessing IC_{50} values in the submicromolar range or less are not common in the literature. In our effort for the discovery of novel inhibitors of CM we have reported a series of *N*-aryl substituted fused triazinone derivatives as potential inhibitors of CM [6]. One of them i.e. compound **A** (Fig. 1) showed weak inhibition of CM (IC_{50} ~ 15.13 ± 0.95 μM). In further continuation of this research we became interested in the identification of fused triazinone based more potent inhibitors **B** (Fig. 2). Our design mainly involved the introduction of a linker "L" at N-3 of the triazinone ring of **A** and replacing the naphthyl ring by an indole moiety of the known inhibitor **C** [7]. We anticipated that apart from introducing the structural flexibility through the linker "L" assembling the structural features of two different inhibitors e.g. **A** and **C** in a single molecular entity i.e. **B** could enhance the overall potency. While a number of compounds can be derived from **C** by varying "L" we focused on simpler moiety like "CH_2" group as "L" at the initial stage.

To verify the merit and potential of our current designing approach, the docking study of three representative molecules e.g. **B-1, B-2** and **B-3** was performed using AutoDock Vina and the binding affinities are presented in Chart 1. All molecules showed better binding affinities than the reference compound **A** [6] and **D** [8] [i.e. 4-(3,4-dimethoxyphenethylamino)-3-nitro-5-sulfamoylbenzoic acid] suggesting their possible superior inhibitory properties against CM [the binding affinity of the most active compound of series represented by **C** is −6.8 Kcal/mol

* Corresponding author.
E-mail address: manojitpal@rediffmail.com (M. Pal).

https://doi.org/10.1016/j.bioorg.2019.103155
Received 26 April 2019; Received in revised form 4 July 2019; Accepted 24 July 2019
Available online 29 July 2019

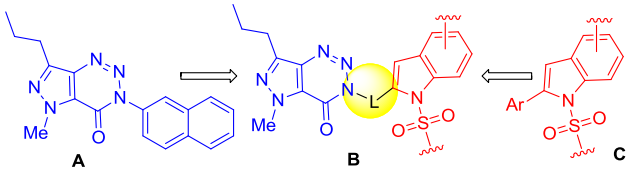

Fig. 1. Design of new triazinone derivative **B** based on known inhibitors **A** and **C**.

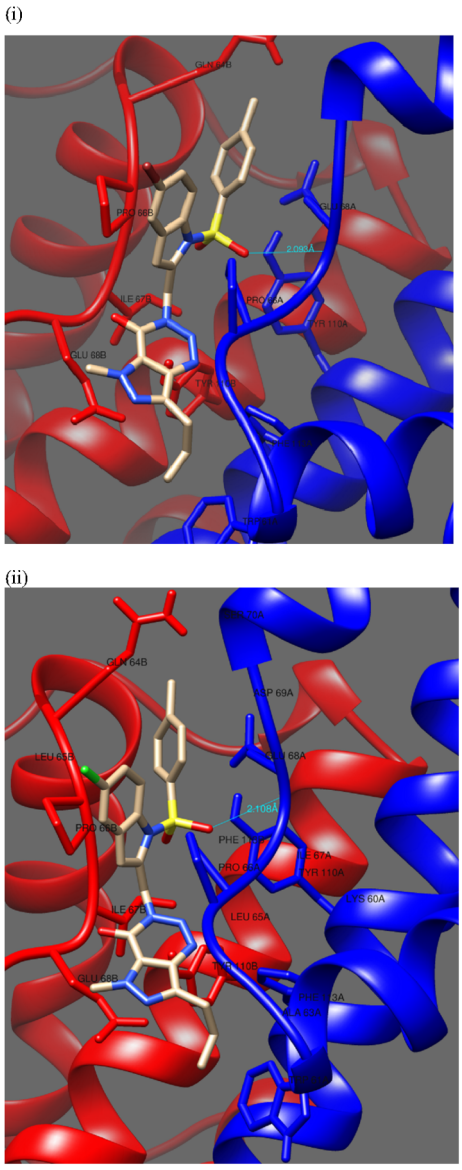

Fig. 2. The 3D interaction diagram of (i) molecule **B-1** and (ii) molecule **B-2** with interface residues of chorismate mutase (PDB code: 2FP2) (the A chain is in blue color, B chain is red, and the H-bond is in cyan color) that were prepared in UCSF Chimera.

(see Fig. S-7 of suppl data file)]. Notably, the docking results showed that the binding energy of these ligands at interface site was lower than the other possible sites of *Mtb*CM (indicating that these molecules were preferably stabilized at the interface site of *Mtb*CM). The compound **B-1** (**3a**) was potentially stabilized (Fig. 2(i), see also suppl data file) by several hydrophobic interactions with the hydrophobic residues (TRP61, LEU65, PRO66, ILE67, TYR110, PHE113 of A chain and LEU65, PRO66, ILE67 of B chain) and hydrophobic regions of polar and charged residues (GLN64, SER 70 of A chain and GLN64, GLU68 of B chain). In addition,

Molecules	Binding affinity (Kcal/mol)
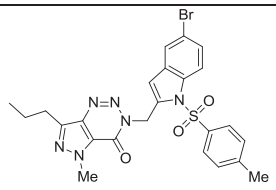 **B-1**	-10.2
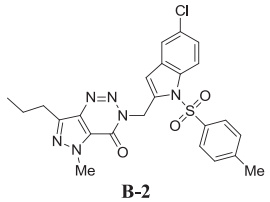 **B-2**	-10.1
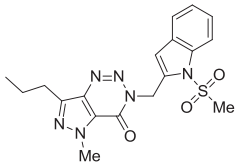 **B-3**	-8.9
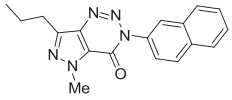 **A**	-6.9
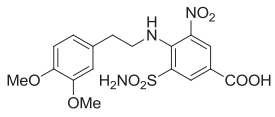 **D**	-7.3

Chart 1. Binding affinities of molecules with *Mtb*CM. ***A** and **D** are known/reference compounds.

residue GLU68 of chain A played vital role to stabilize the docked complex through H-bonding (formed between its nitrogen atom of GLU68 and the sulfonyl oxygen of **B-1**) in the distance of 2.093 Å.

Like **B-1** the molecule **B-2** also formed H-bond through its sulfonyl oxygen with the nitrogen atom of the GLU68 of A chain in the distance of 2.108 Å (Fig. 2(ii)). However, the positive charged residue LYS60 of A chain made a hydrophobic contact here that was not observed in case of **B-1**. While the similar H-bonding was observed for **B-3** (see suppl data file) too (involving its sulfonyl oxygen and the nitrogen atom of the GLU68A of A chain in the distance of 2.107 Å) some of the hydrophobic contacts with residues like ILE67A, SER70A, GLN64B, and PHE113B were missing in this case perhaps due to the less hydrophobicity of **B-3** (compared to the previous molecules) thereby accounting for its marginally low binding affinity (Chart 1). Nevertheless, the overall outcome of *in silico* study appeared to be promising and hence prompted us to undertake the actual synthesis as well as *in vitro* evaluation of compounds based on framework **B** (Fig. 1) including **B-1**, **B-2** and **B-3**. Herein we report the preliminary results of our study that allowed us to discover a new class of CM inhibitors which to our knowledge has not been explored earlier.

2. Results and discussion

2.1. Chemistry

The designed compounds were conveniently prepared following a coupling-cyclization strategy under Pd/Cu-catalysis. Indeed, the transition metal mediated coupling/cyclization in the same pot [7,9–11] has become a common strategy for the synthesis of 2-substituted indoles [12]. This one-pot reaction typically involves the use of terminal

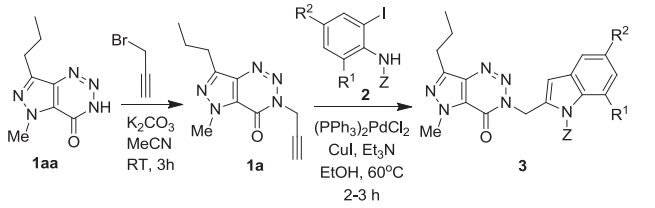

Scheme 1. Synthesis of 3-indolylmethyl substituted pyrazolotriazinone derivatives **3.**

Table 1
Effect of reaction conditions on coupling of terminal alkyne **1a** with **2a**.[a]

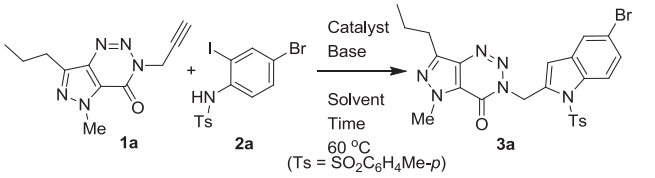

.

Entry	Catalyst (10 mol%)	Base	Solvent	Time (h)	%Yield[b]
1	CuI	K_2CO_3	PEG-400	8	15
2	CuI	Et_3N	PEG-400	8	0
3	CuI	K_2CO_3	EtOH	8	20
4	$InCl_3$	K_2CO_3	EtOH	8	0
5[c]	CuI/$InCl_3$	K_2CO_3	EtOH	8	20
6[c]	CuI/ PPh_3 10%Pd/C	K_2CO_3	EtOH	8	40
7[c]	CuI/ PPh_3 10%Pd/C	Et_3N	EtOH	8	65
8[d]	CuI $Pd(PPh_3)_2Cl_2$	Et_3N	EtOH	2	82
9[d]	CuI $Pd(PPh_3)_2Cl_2$	K_2CO_3	H_2O	8	0
10[c]	CuI/ PPh_3 10%Pd/C	K_2CO_3	H_2O	8	0

[a] Reactions were carried out using alkyne **1a** (1 mmol), **2a** (1.2 mmol), base (2.0 mmol) and catalyst in a solvent (10 mL) under nitrogen at 60 °C.
[b] Isolated yield.
[c] 10 mol% of each catalyst used.
[d] 1 mol% of each catalyst used.

alkynes as key reactants that are coupled with a 2-iodoanilide. The terminal alkyne i.e. 5-methyl-3-(prop-2-ynyl)-7-propyl-3*H*-pyrazolo [4,3-*d*][1,2,3] triazin-4(5*H*)-one (**1a**) required in the current study was prepared following a known method and were coupled with appropriate 2-iodosulphanilides (**2**) under Pd/Cu-catalysis (Scheme 1).

Initially, the alkyne **1a** was reacted with *N*-(4-bromo-2-iodophenyl)-4-methylbenzenesulfonamide **2a** in the presence of CuI and K_2CO_3 in PEG-400 at 60 °C for 8 h (Table 1). While the expected product **3a** was isolated in this case the yield was poor (entry 1, Table 1). The change of base to Et_3N (entry 2, Table 1) or solvent to EtOH (entry 3, Table 1) did not improve the yield. The use of other catalyst e.g. $InCl_3$ (entry 4, Table 1) or combination of CuI and $InCl_3$ (entry 5, Table 1) was also found to be not effective. The product yield was improved to some extent when combination of 10%Pd/C-CuI-PPh_3 was used as a catalyst system along with K_2CO_3 as a base (entry 6, Table 1).

Indeed, further improvement in yield was observed when K_2CO_3 was replaced by Et_3N (entry 7, Table 1). Interestingly, a substantial increase in yield was observed when the combination of $(PPh_3)_2PdCl_2$-CuI was used as a catalyst system along with Et_3N as a base (entry 8, Table 1). Notably 10 mol% of each catalyst was used in all the cases earlier (entries 1–7, Table 1) whereas only 1 mol% of $(PPh_3)_2PdCl_2$ and CuI each was necessary in the case of entry 8 of Table 1 (indeed, the increase of catalysts quantity did not improve the product yield whereas use of < 1 mol% of catalysts decreased the yield. For further details, see: Table S-1, suppl data file). Though the use of water as a cheap and non-hazardous solvent was not successful in this case (entry 9, Table 1) we were satisfied with the %yield of **3a** obtained in case of entry 8 of Table 1. Thus the use of $(PPh_3)_2PdCl_2$-CuI and Et_3N in EtOH was found to be optimal for the preparation of **3a** and was used to prepare other related analogues (Scheme 1, Table 2, see also Table S-2, suppl data file). A number of 2-iodosulphanilides (**2a-k,** Z = mesyl, tosyl, phenylsulfonyl, 2-thienosulfonyl) were reacted with alkyne **1a** under the optimized conditions. The reaction proceeded well irrespective of the presence of various substituents [e.g. F (**3f**), Cl (**3b, 3d, 3h**), Br (**3a**), NO_2 (**3j**) and Me (**3k**)] affording the desired 3-indolylmethyl substituted pyrazolotriazinone derivatives in good yields.

Table 2
Preparation[a] of compound **3** (Scheme 1) and their *in vitro* evaluation against CM.

Entry	R^1 = ; R^2 =; Z = (**2**)	**3**[b]	%Yield[c]	% inhibition[d] @30 μM
1	H, Br, Ts (**2a**)	**3a**	82	ND
2	H, Cl, Ms (**2b**)	**3b**	78	5
3	H, H, SO_2Ph (**2c**)	**3c**	72	25
4	H, Cl, Ts (**2d**)	**3d**	78	70
5	H, H, Ts (**2e**)	**3e**	80	20
6	H, F, Ts (**2f**)	**3f**	74	7
7	H, H, Ms (**2g**)	**3g**	76	37
8	H, Cl, 2-Thienosulfonyl (**2h**)	**3h**	78	ND
9	H, H, 2-Thienosulfonyl (**2i**)	**3i**	78	24
10	H, NO_2, Ms (**2j**)	**3j**	80	30
11	H, Me, Ts (**2k**)	**3k**	72	19

*Ms = mesyl, Ts = *p*-tosyl, ND = Not determined.
[a] All the reactions were carried out using alkyne **1a** (1 mmol), **2** (1.2 mmol), $(PPh_3)_2PdCl_2$ (1 mol%), CuI (1 mol%), and Et_3N (2 mmol) in EtOH (10 mL) at 60 °C for 2–3 h.
[b] Identified by ^1H and ^{13}C NMR, IR, and MS.
[c] Isolated yields.
[d] Compound **A** and **D** showed 38% and 57% inhibition at 30 μM.

Having prepared a range of pyrazolotriazinone containing novel indole derivatives (**3**) we focused on assessing generality of the present Pd/Cu-catalyzed coupling-cyclization reaction by using simpler alkyne (**1b**) derived from **1a** e.g. replacing the pyrazole moiety of **1a** by a benzene ring (i.e. the benzo analogue to **1a**). Accordingly, **1b** was prepared from benzo[*d*][1,2,3]triazin-4(3*H*)-one (**1bb**) and employed in the Pd/Cu-catalyzed coupling-cyclization with a number of 2-iodoanilides (**2**) under the optimized conditions (entry 8, Table 1). The corresponding indoles i.e. 3-indolylmethyl substituted benzotriazinone derivatives (**4a-l**) were obtained in good yields in all these cases (Table 3, see also Table S-2, suppl data file). Indeed, the use of three additional anilides (**2l-n**) was also successful when the desired products were isolated in good yields (entries 10–12, Table 3). Finally, the use of 6-bromo-3-(prop-2-yn-1-yl)benzo[*d*][1,2,3]triazin-4(3*H*)-one (**1c**) [prepared from 6-bromobenzo[*d*][1,2,3]triazin-4(3*H*)-one (**1cc**), see suppl data file] was examined that afforded the corresponding indole derivative (**4m**) when coupled with the **2d** (entry 13, Table 3).

All the synthesized 3-indolylmethyl substituted pyrazolo and benzotriazinone derivatives (**3** and **4**) were characterized by (^1H and ^{13}C NMR, and MS) spectral data. Briefly (Fig. 3), a singlet near δ 6.1 and 6.0 in the ^1H NMR spectra accounted for the linker "CH_2" moiety and C-3 indole proton, respectively. The compound **3** was further characterized by the presence of NCH_3 protons near δ 4.3 and the *n*-propyl moiety near δ 3.0 (t, CH_2), 1.9–1.8 (m, CH_2) and 1.0 (t, CH_3). The "C═O" group of the fused triazinone moiety appeared in the region 150–155 ppm in ^{13}C NMR spectra and showed a strong IR absorption in the region 1700–1670 cm^{-1}.

Mechanistically (Scheme 2) [9,10,11], the present coupling-cyclization method proceeded via (i) a first catalytic cycle i.e. the known Sonogashira coupling [13] involving *in situ* generated Pd(0) catalysed C−C bond forming reaction to give the alkyne **E-1** followed by (ii) the

Table 3
Preparation[a] of compound **4** and their *in vitro* evaluation against CM.

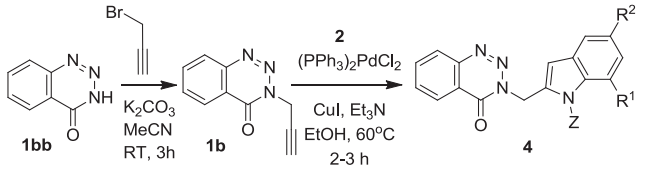

.

Entry	R^1 =; R^2 =; Z = (**2**)	**4**[b]	Yield[c]	% inhibition[d] @30 μM
1	H, Br, Ts (**2a**)	**4a**	80	38
2	H, Cl, Ms (**2b**)	**4b**	78	26
3	H, H, SO_2Ph (**2c**)	**4c**	74	42
4	H, Cl, Ts (**2d**)	**4d**	81	78
5	H, H, Ts (**2e**)	**4e**	77	56
6	H, F, Ts (**2f**)	**4f**	71	41
7	H, H, Ms (**2g**)	**4g**	80	20
8	H, Cl, 2-Thienosulfonyl (**2h**)	**4h**	80	57
9	H, H, 2-Thienosulfonyl (**2i**)	**4i**	78	45
10	H, F, Ms (**2l**)	**4j**	72	29
11	Me, Me, Ms (**2m**)	**4k**	68	37
12	Me, Me, SO_2Ph (**2n**)	**4l**	66	27
13	H, Cl, Ts (**2d**)	**4m**	79[e]	34

*Ms = mesyl, Ts = *p*-tosyl, ND = Not determined.

[a] All the reactions were carried out using alkyne **1b** (1 mmol), **2** (1.2 mmol), $(PPh_3)_2PdCl_2$ (1 mol%), CuI (1 mol%), and Et_3N (2 mmol) in EtOH (10 mL) at 60 °C for 2–3 h.

[b] Identified by ^{1}H and ^{13}C NMR, IR, and MS.

[c] Isolated yields.

[d] Compound **A** and **D** showed 38% and 57% inhibition at 30 μM

[e] 6-bromo-3-(prop-2-yn-1-yl)benzo[*d*][1,2,3]triazin-4(3*H*)-one (**1c**) was used in place of **1b** and the corresponding product obtained was 6-bromo-3-{(5-chloro-1-tosyl-1*H*-indol-2-yl)methyl}benzo[*d*][1,2,3]triazin-4(3*H*)-one (**4m**).

second catalytic cycle i.e. Cu(I)-catalysed intramolecular cyclization of **E-1** to give the desired fused triazinone containing indole derivatives **3** or **4**. The second catalytic cycle proceeded via interaction of Cu(I) with the alkyne moiety of **E-1** that seemed to be favoured by the coordination with the proximate carbonyl group (of **E-2**) leading to **E-3**. Protonolysis of the organo-copper species **E-3** afforded the desired product via **E-4** with the regeneration of CuI to complete the second catalytic cycle (the cyclization step).

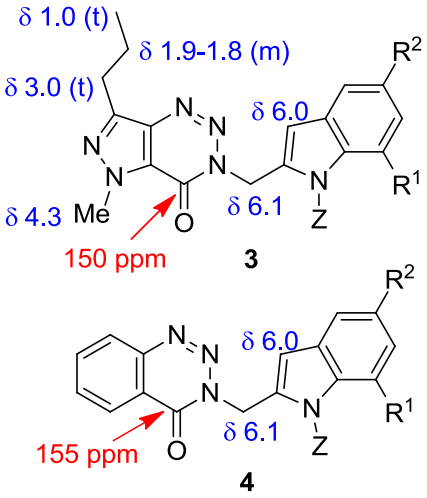

Fig. 3. Partial ^{1}H and ^{13}C NMR data of compound **3** and **4**.

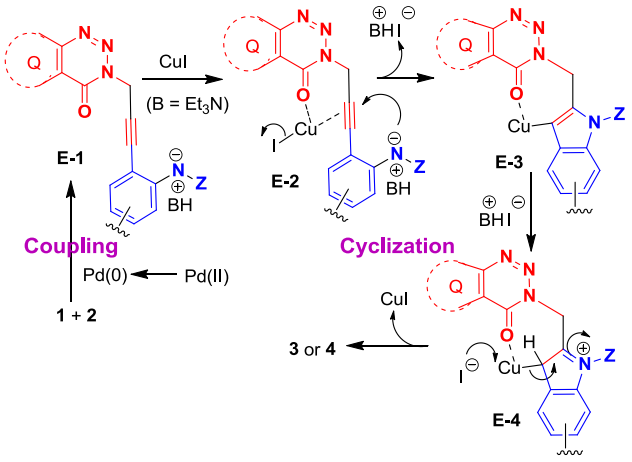

Scheme 2. The plausible reaction mechanism for coupling-cyclization of fused triazinone alkyne (**1**) with 2-iodoanilides (**2**) under Pd/Cu-catalysis.

2.2. Biology

We then tested all the synthesized compounds i.e. **3** and **4** for their CM inhibitory properties *in vitro* [14] using an assay that involved measurement of catalytic activity of enzyme (CM) in the conversion of chorismate (substrate) to prephenate. The known inhibitor [8] **D** (Chart 1) was used as a reference compound. All compounds were tested at an initial concentration of 30 μM and compounds showed inhibition > 50% were identified as most active inhibitors of CM. In case of pyrazolotriazinone series (**3**) the compound **3d** showed significant inhibition (Table 2) whereas compound **4d**, **4e** and **4h** from the benzotriazinone series were identified as most active inhibitors (Table 3). Several other compounds showed moderate inhibition (~35–40%) from both series e.g. **3g** (Table 2), **4a**, **4c**, **4f**, **4i** and **4k** (Table 3). Notably, greater number of compounds from benzotriazinone series was found to be active compared to that of pyrazolotriazinone series partially due to the fact that compounds from the later series showed some solubility issue in the assay medium used. For example compound **3a** and **3h** could not be tested because of their precipitation in the assay medium. Indeed, compound **3** was expected to be more lipophilic than **4** due to the presence of more number of nitrogen atoms and alkyl side chains. Nevertheless, an overview of SAR (Structure-Activity-Relationship) observations noted from the current series of compounds is summarized in Fig. 4. In general the "Cl" group at C-5 of indole ring was beneficial for CM inhibition whereas other substituents like F, Br or Me or no substituent at this position decreased the activity. No substituent at C-7 position was generally favorable whereas a "Me" group at the same position lowered the activity. Among the sulfonyl substituents at indole N-1 position the *p*-tosyl group contributed towards high activity though low activity was also observed in few cases. The other groups like mesyl, phenylsulfonyl and 2-thienosulfonyl groups were found to be inferior. The aryl/heteroaryl ring fused with the triazinone moiety also influenced the activity. This is exemplified by the fact that three compounds (e.g. **4d**, **4e** and **4h**) showed inhibition > 50% contain benzene ring fused with the triazinone moiety whereas only one compound (**3d**) showed high activity that contains pyrazole ring at the same place.

Nonetheless, the best active compounds i.e. **3d** from the pyrazolotriazinone series and **4d** from the benzotriazinone series were taken forward for concentration dependent study to determine their IC_{50} values. Accordingly, the IC_{50} values were found to be 0.40 ± 0.05 μM (Fig. 5) and 0.85 ± 0.10 μM for compound **3d** and **4d**, respectively whereas that of known compound **D** was 5.3 ± 0.2 μM. It was therefore evident that both the compounds were more potent than **D** in this assay. Moreover, the current efforts afforded better active fused

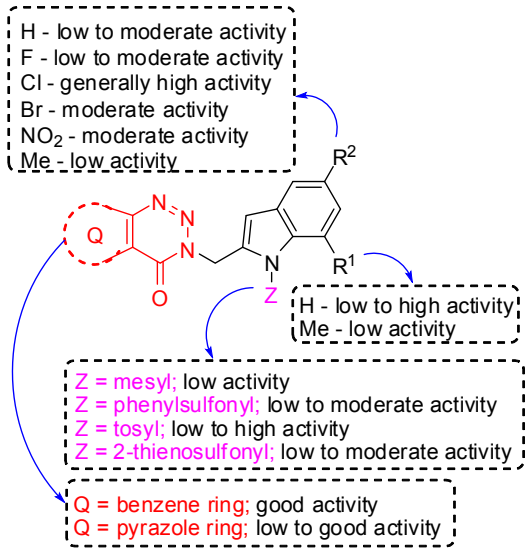

Fig. 4. Summary of SAR for CM inhibitory activities of compound **3** and **4**.

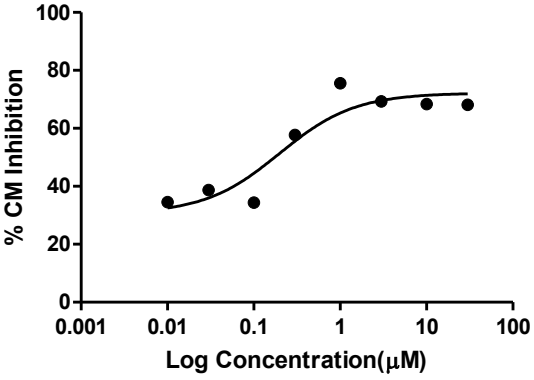

Fig. 5. Concentration dependent study of compound **3d** against CM.

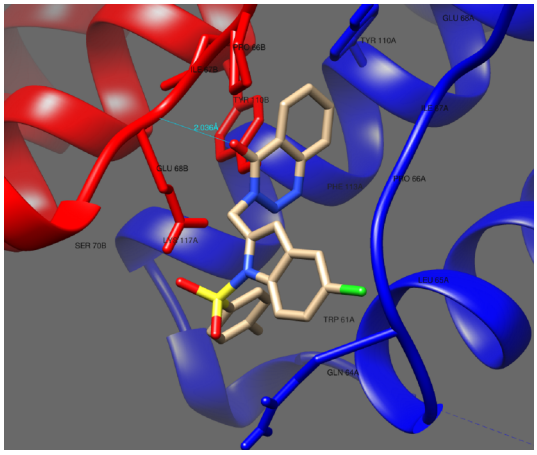

Fig. 6. The 3D interaction diagram of compound **4d** with interface residues of chorismate mutase (PDB code: 2FP2).

triazinone derivatives than the previously reported inhibitor **A** (Fig. 1) [6]. These compounds were also evaluated for their potential toxicity by MTT assay on RAW 264.7 cell line (a commonly used model of mouse macrophages for the study of cellular responses to microbes and their products) at different concentrations. None of them showed significant toxicities till 30 μM of their concentration tested. Indeed, % cell viability was found to be 100, 100, 86, 91, 68 and 42% at the concentration of 1, 3, 10, 30, 60 and 100 μM of **3d**, respectively suggesting potential/acceptable therapeutic window for this compound.

To understand the interaction of these molecules with CM through *in silico* studies it was desirable to analyze and compared the docking results. Since the docking results of compound **3d** was already available (molecule **B-2**, Fig. 2(ii)) hence docking of **4d** was performed. According to the docking results (Fig. 6) compound **4d** (binding affinity −9.5 Kcal/mol) was potentially stabilized by several hydrophobic interactions with the hydrophobic residues (TRP61, LEU65, PRO66, ILE67, TYR110, PHE113 of A chain and PRO66, ILE67, TYR110 of B chain) and hydrophobic regions of polar and charged residues (GLN64 of A chain and GLU68 of B chain). Unlike **3d** the compound **4d** (being a benzotriazinone derivative rather than pyrazolotriazinone) was stabilized by a slightly different binding mode at the interface site, and formed H-bond at a distance of 2.036 Å with the residue GLU68 of chain B instead of chain A.

Since the early detection of ADME (absorption, distribution, metabolism, and excretion) or pharmacokinetic properties of NCEs (new chemical entities) is an useful strategy for further progress of molecules hence computational ADME prediction of compounds **3d** and **4d** along with the known inhibitor **D** was performed using SwissADME web-tool [15] and results are presented in Table 4 (among the various descriptors only notable one are listed in the table). In spite of one violation of Lipinski's criteria (molecular weight > 500) the desirable ADME was predicted for compound **3d**. The desirable ADME was predicted for **4d** too with no such violation. Indeed, high GI absorption, no BBB (Blood Brain Barrier) penetration and no P-gp substrate potential have been predicted for both molecules with superior bioavailability score over the reference molecule **D**. Overall, the compound **3d** and **4d** could be better inhibitors than **D** and appeared to have medicinal value especially from the viewpoint of developing potential antitubercular agents. Notably, favorable biological properties of 1,2,3-benzotriazin-4-one derivatives have been documented well in the literature [16]. The compound **3d** and **4d** therefore deserves further pharmacological profiling.

3. Conclusion

In conclusion, a series of novel 3-indolylmethyl substituted pyrazolotriazinone derivatives were initially designed and docked into CM *in silico* as potential inhibitors of CM. Synthesis of these compounds were carried out efficiently using the Pd/Cu-catalyzed coupling-cyclization in a single pot involving the construction of indole ring. The methodology involved reaction of 5-methyl-3-(prop-2-ynyl)-7-propyl-3*H*-pyrazolo[4,3-*d*][1,2,3]triazin-4(5*H*)-one with a number of 2-iodosulphanilides in the presence of $(PPh_3)_2PdCl_2$, CuI and Et_3N in EtOH at 60 °C for 2–3 h to afford the desired compounds in good yields. The methodology was later extended to the preparation of corresponding benzene analogs of pyrazolotriazinones i.e. 3-indolylmethyl substituted benzotriazinone derivatives. Overall, more than 20 new compounds were prepared and tested for their CM inhibitory potentials *in vitro*. Several of these compounds showed significant inhibition of CM when tested at 30 μM. The SAR (Structure-Activity-Relationship) studies suggested that benzotriazinone moiety was more favorable over the pyrazolotriazinone ring. The two best active compounds showed IC_{50} values ~0.4–0.9 μM and were found to be more potent than the reference/known compounds used. They were also non-toxic towards RAW 264.7 cell line till 30 μM in an MTT assay. The present 3-indolylmethyl substituted (pyrazolo/benzo)triazinone framework appeared to be an useful template for the design, synthesis and identification of potent inhibitors of CM.

Table 4
Computational ADME prediction of **3d**, **4d** and **D**.

Properties	Molecules		
(i) Physicochemical	**3d**	**4d**	**D**
Molecular Weight (g/mol)	511.00	464.92	425.41
Consensus Log P[a]	4.41	4.55	0.90
Log S (ESOL)[b]	−6.41 (poorly soluble)	−6.44 (poorly soluble)	−3.63 (soluble)
(ii) Pharmacokinetics			
GI[c] absorption	High	High	Low
BBB[d] permeation	No	No	No
P-gp[e] substrate	No	No	Yes
(iii) Druglikenss			
Lipinski rule	1 violation: MW[f] > 500	No violation	No violation
Veber rule	No violation	No violation	1 violation (TPSA[g] > 140; i.e. 182.15 Å^2)
Bioavailability score	0.17	0.55	0.11

[a] Log P: Lipophilicity.
[b] Log S (ESOL): water solubility, calculated by ESOL method which Quantitative Structure-Property Relationship (QSPR) based model.
[c] GI: Gastrointestinal.
[d] BBB: Blood Brain Barrier.
[e] P-gp: permeability glycoprotein.
[f] MW: molecular weight,
[g] TPSA: Topological polar surface area.

4. Experimental section

4.1. Chemistry

4.1.1. General methods

Unless stated otherwise, reactions were performed under nitrogen atmosphere using oven dried glassware. Reactions were monitored by thin layer chromatography (TLC) on silica gel plates (60 F254), visualizing with ultraviolet light or iodine spray. Flash chromatography was performed on silica gel (230–400 mesh) using distilled hexane and EtOAc. ^{1}H and ^{13}C NMR spectra were recorded in $CDCl_3$ or DMSO-d_6 solution by using a 400 and 100 MHz spectrometer. Proton chemical shifts (δ) are relative to tetramethylsilane (TMS, $\delta = 0.00$) as internal standard and expressed in ppm. Spin multiplicities are given as s (singlet), d (doublet), dd (doublet of doublet), td (triplet of doublet), t (triplet) and m (multiplet) as well as bs (broad singlet). Coupling constants (*J*) are given in hertz. Melting points were determined using melting point apparatus and are uncorrected. MS spectra were obtained on Agilent 6430 series Triple Quard LC-MS/MS spectrometer. Chromatographic purity by HPLC (Agilent 1200 series ChemStation software) was determined by using area normalization method and the condition Specified in each case: column, mobile phase (range used), flow rate, detection wavelength, and retention times. The starting compound **1aa** and **1bb** was prepared following a reported method [6, 16a].

4.1.2. General procedure for the preparation of compound *1a-c*

Propargyl bromide (1.2 mmol) was added to a solution of **1aa** or **1bb** or **1cc** (1.0 mmol) and K_2CO_3 (3.0 mmol) in CH_3CN (25 mL) under a nitrogen atmosphere. The mixture was stirred at room temperature for 3 h. After completion of the reaction (confirmed by TLC), the mixture was diluted with ice-water (60 mL) and extracted with EtOAc (3 × 15 mL). The organic layers were collected, combined, dried over anhydrous Na_2SO_4, filtered and concentrated under low vacuum. The residue was purified by column chromatography using hexane- EtOAc as eluent to afford the title compound.

4.1.3. 5-Methyl-3-(prop-2-yn-1-yl)-7-propyl-3H-pyrazolo[4,3-d][1,2,3]triazin-4(5H)-one (*1a*)

White solid (78% yield); mp 55–57 °C; R_f (20% EtOAc/*n*-hexane) 0.3; ^{1}H NMR (400 MHz, $CDCl_3$) δ: 5.19 (d, J = 2.4 Hz, 2H, NCH_2), 4.29 (s, 3H, NCH_3), 3.01(t, J = 7.6 Hz, 2H, CH_2), 2.37 (t, J = 2.4 Hz, 1H, HC≡C), 1.93–1.82 (m, 2H, $MeCH_2$), 1.01 (t, J = 7.6 Hz, 3H, CH_3); ^{13}C NMR (100 MHz, $CDCl_3$) δ: 149.8 (C═O), 148.6, 136.1, 124.7, 77.0 (-C≡), 73.2 (HC≡), 38.8 (CH_2), 38.6 (NMe), 27.8 (CH_2), 22.3 (CH_2), 13.9 (Me); IR (KBr) ν_{max} 3238, 2120, 1697, 1531 cm^{-1}; MS (ES mass): *m/z* 232.2 (M + 1, 100%).

4.1.4. 3-(Prop-2-yn-1-yl)benzo[d][1,2,3]triazin-4(3H)-one (*1b*)

White solid (80% yield); mp 103–105 °C; R_f (20% EtOAc/*n*-hexane) 0.35; ^{1}H NMR (400 MHz, $CDCl_3$) δ: 8.38 (dd, J = 8.0, 1.2 Hz, 1H, ArH), 8.18 (d, J = 8.4 Hz, 1H, ArH), 8.01–7.94 (m, 1H, ArH), 7.85–7.80 (m, 1H, ArH),5.23 (d, J = 2.8 Hz, 2H, NCH_2), 2.38 (t, J = 2.8 Hz, 1H, HC≡C); ^{13}C NMR (100 MHz, $CDCl_3$) δ: 154.9(C═O), 144.3, 135.1, 132.7, 128.5, 125.2, 119.9, 76.9 (-C≡), 73.3 (HC≡), 39.4 (CH_2); MS (ES mass): *m/z* 186.20 (M + 1, 100%).

4.1.5. 6-Bromo-3-(prop-2-yn-1-yl)benzo[d][1,2,3]triazin-4(3H)-one (*1c*)

White solid (75% yield); mp 92–94 °C; R_f (20% EtOAc/*n*-hexane) 0.4; ^{1}H NMR (400 MHz, $CDCl_3$) δ: 8.12–7.95 (m, 2H, ArH), 8.51 (s, 1H, ArH), 5.21 (d, J = 2.8 Hz, 2H, NCH_2), 2.38 (t, J = 2.8 Hz, 1H, HC≡C); ^{13}C NMR (100 MHz, $CDCl_3$) δ: 153.6 (C═O), 142.9, 138.5, 130.2, 128.0, 127.4, 121.2, 76.6 (-C≡), 73.5 (HC≡), 39.5 (CH_2); HPLC: 99.5%, column: X Bridge C-18 150*4.6 mm 5 µm, mobile phase A: 5 mM Ammonium Acetate in water, mobile phase B: CH_3CN, (gradient) T/B% : 0/10, 23/90, 30/90, 31/90, 35/10; flow rate: 1 mL/min; Max plot, retention time 13.6 min; MS (ES mass): *m/z* 265.9 (M + 2, 100%).

4.1.6. General procedure for the preparation of compound *3* and *4*

A mixture of compound **1a** or **1b** or **1c** (1.0 mmol), 2-iodosulphanilides (**2**, 1.2 mmol), $(PPh_3)_2PdCl_2$ (1 mol%), CuI (1 mol%) and Et_3N (2.0 mmol) in EtOH (10 mL) was stirred at 60 °C for 2–3 h. After completion of the reaction (indicated by TLC) the reaction mixture is diluted with EtOAc (50 mL) and filtered through celite bed. The organic layer was collected, washed with water (3 × 30 mL), dried over anhydrous Na_2SO_4, filtered and concentrated under low vacuum. The crude residue was purified by column chromatography on silica gel using hexane-EtOAc to afford the desired product.

4.1.7. 3-{(5-Bromo-1-tosyl-1H-indol-2-yl)methyl}-5-methyl-7-propyl-3H-pyrazolo[4,3-d][1,2,3]triazin-4(5H)-one (*3a*)

White solid (82% yield); mp: 170–172 °C; R_f (20% EtOAc/*n*-hexane) 0.24; ^{1}H NMR (400 MHz, $CDCl_3$) δ: 7.95 (d, J = 8.8 Hz, 1H, ArH), 7.79 (d, J = 8.4 Hz, 2H, ArH), 7.44 (d, J = 1.7 Hz, 1H, ArH), 7.36 (dd, J = 8.8, 2 Hz, 1H, ArH), 7.27 (d, J = 8.4 Hz, 2H, ArH), 6.06 (s, 2H, NCH_2), 6.01 (s, 1H, indole (C-3) H), 4.30 (s, 3H, NCH_3), 3.05 (t,

J = 7.6 Hz, 2H, CH_2), 2.36 (s, 3H, $ArCH_3$), 1.97–1.86 (m, 2H, $MeCH_2$), 1.05 (t, J = 7.6 Hz, 3H, CH_3); ^{13}C NMR (100 MHz, $CDCl_3$) δ: 150.2 (C═O), 148.6, 145.5, 136.9, 136.1, 135.7, 135.0, 130.9, 130.1 (2C), 127.6, 126.6 (2C), 124.6, 123.4, 117.2, 115.9, 108.8, 46.8 (NCH_2), 38.8 (NMe), 27.9 (CH_2), 22.3 (CH_2), 21.6 (ArMe), 14.0 (Me); HPLC: 98.9%, column: X Bridge C-18 150 * 4.6 mm 3.5 µm, mobile phase A: 0.1% TFA in water, mobile phase B: CH_3CN:THF (80:20), (gradient) T/B% : 0/10, 20/95, 40/95, 41/10, 45/10; flow rate: 1 mL/min; UV 220.0 nm, retention time 18.6 min; IR (KBr) ν_{max} 2965, 1706, 1533, 1402 cm^{-1}; MS (ES mass): m/z 557.1 (M + 2, 100%), 555.1 (M^+, 98%).

*4.1.8. 3-[{5-Chloro-1-(methylsulfonyl)-1H-indol-2-yl}methyl]-5-methyl-7-propyl-3H-pyrazolo[4,3-d][1,2,3]triazin-4(5H)-one (**3b**)*

White solid (78% yield); mp: 141–143 °C; R_f (20% EtOAc/*n*-hexane) 0.24; ^{1}H NMR (400 MHz, $CDCl_3$) δ: 7.95 (d, J = 8.8 Hz, 1H, ArH), 7.42 (d, J = 2 Hz, 1H, ArH), 7.29 (dd, J = 8.8, 2 Hz, 1H, ArH), 6.27 (s, 1H, indole (C-3) H), 5.96 (s, 2H, NCH_2), 4.28 (s, 3H, NCH_3), 3.31 (s, 3H, SCH_3), 3.04 (t, J = 7.6 Hz, 2H, CH_2), 1.93–1.87 (m, 2H, $MeCH_2$), 1.04 (t, J = 7.6 Hz, 3H, CH_3); ^{13}C NMR (100 MHz, $CDCl_3$) δ: 150.1 (C═O), 148.6, 136.9, 136.2, 135.0, 130.2, 129.7, 125.2, 124.6, 120.5, 115.0, 109.2, 45.9 (NCH_2), 41.2 (SMe), 38.8 (NMe), 27.9 (CH_2), 22.3 (CH_2), 14.0 (Me); HPLC: 99.9%, column: X Bridge C-18 150 * 4.6 mm 5 µm, mobile phase A: 0.1% TFA in water, mobile phase B: CH_3CN, (gradient) T/B% : 0/30, 20/95, 30/95, 31/30, 35/30; flow rate: 1 mL/min; max plot, retention time 14.8 min; IR (KBr) ν_{max} 3006, 1697, 1533, 1446 cm^{-1}; MS (ES mass): m/z 435.1 (M + 1, 100%).

*4.1.9. 5-Methyl-3-{(1-(phenylsulfonyl)-1H-indol-2-yl)methyl}-7-propyl-3H-pyrazolo[4,3-d][1,2,3]triazin-4(5H)-one (**3c**)*

White solid (72% yield); mp: 154–156 °C; R_f (20% EtOAc/*n*-hexane) 0.24; ^{1}H NMR (400 MHz, $CDCl_3$) δ: 8.07 (d, J = 8.4 Hz, 1H, ArH), 7.97–7.88 (m, 2H, ArH), 7.57–7.52 (m, 1H, ArH), 7.46 (t, J = 8 Hz, 2H, ArH), 7.33 (d, J = 8 Hz, 1H, ArH), 7.30–7.24 (m, 1H, ArH), 7.20–7.14 (m, 1H, ArH), 6.10 (s, 1H, indole (C-3) H), 6.08 (s, 2H, NCH_2), 4.30 (s, 3H, NCH_3), 3.05 (t, J = 7.6 Hz, 2H, CH_2), 1.97–1.87 (m, 2H, $MeCH_2$), 1.05 (t, J = 7.6 Hz, 3H, CH_3); ^{13}C NMR (100 MHz, $CDCl_3$) δ: 150.2 (C═O), 148.6, 138.3, 137.0, 135.5, 133.9, 129.4 (2C), 129.2, 126.6 (2C), 124.8, 124.7, 123.8, 120.8, 116.7, 114.4, 110.0, 46.8 (NCH_2), 38.8 (NMe), 27.9 (CH_2), 22.3 (CH_2), 14.0 (Me); HPLC: 98.9%, column: Eclips XDB C-18 150 * 4.6 mm 5 µm, mobile phase A: 0.05% TFA in water, mobile phase B: 0.05% TFA in CH_3CN, (gradient) T/B% : 0/10, 5/10, 25/90, 30/90, 31/10, 35/10; flow rate: 1 mL/min; UV 218.0 nm, retention time 24.8 min; IR (KBr) ν_{max} 2953, 1707, 1529, 1475 cm^{-1}; MS (ES mass): m/z 463.1 (M + 1, 100%).

*4.1.10. 3-{(5-Chloro-1-tosyl-1H-indol-2-yl)methyl}-5-methyl-7-propyl-3H-pyrazolo[4,3-d][1,2,3]triazin-4(5H)-one (**3d**)*

White solid (78% yield); mp: 151–153 °C; R_f (20% EtOAc/*n*-hexane) 0.24; ^{1}H NMR (400 MHz, $CDCl_3$) δ: 7.98 (d, J = 8.8 Hz, 1H, ArH), 7.78 (d, J = 8 Hz, 2H, ArH), 7.27–7.22 (m, 3H, ArH), 7.22–7.17 (m, 1H, ArH), 6.04 (s, 2H, NCH_2), 6.01 (s, 1H, indole (C-3) H), 4.28 (s, 3H, NCH_3), 3.03 (t, J = 7.6 Hz, 2H, CH_2), 2.33 (s, 3H, $ArCH_3$), 1.96–1.85 (m, 2H, $MeCH_2$), 1.04 (t, J = 7.6 Hz, 3H, CH_3); ^{13}C NMR (100 MHz, $CDCl_3$) δ: 150.2 (C═O), 148.6, 145.5, 137.2, 136.1, 135.3, 135.0, 130.4, 130.1 (2C), 129.5, 126.6 (2C), 124.9, 124.6, 120.3, 115.5, 108.9, 46.8 (NCH_2), 38.8 (NMe), 27.9 (CH_2), 22.3 (CH_2), 21.6 (ArMe), 14.0 (Me); HPLC: 99.9%, column: Cosmicsil Aura ODS C-18 150 * 4.6 mm 5 µm, mobile phase A: 0.1% TFA in water, mobile phase B: CH_3CN, (gradient) T/B% : 0/10, 20/95, 27/95, 31/10, 35/10; flow rate: 1 mL/min; UV 220.0 nm, retention time 21.2 min; IR (KBr) ν_{max} 2960, 1705, 1532, 1403 cm^{-1}; LCMS : m/z 511.1 (M + 1, 100%).

*4.1.11. 5-Methyl-7-propyl-3-{(1-tosyl-1H-indol-2-yl)methyl}-3H-pyrazolo [4,3-d][1,2,3]triazin-4(5H)-one (**3e**)*

White solid (80% yield); mp: 151–153 °C; R_f (20% EtOAc/*n*-hexane) 0.24; ^{1}H NMR (400 MHz, $CDCl_3$) δ: 8.07 (d, J = 8.4 Hz, 1H, ArH), 7.81 (d, J = 8.4 Hz, 2H, ArH), 7.34–7.22 (m, 4H, ArH), 7.18–7.14 (m, 1H, ArH), 6.08 (bs, 3H, NCH_2, indole (C-3) H), 4.30 (s, 3H, NCH_3), 3.05 (t, J = 7.6 Hz, 2H, CH_2), 2.33 (s, 3H, $ArCH_3$), 1.97–1.86 (m, 2H, $MeCH_2$), 1.05 (t, J = 7.6 Hz, 3H, CH_3); ^{13}C NMR (100 MHz, $CDCl_3$) δ: 150.2 (C═O), 148.6, 145.1, 137.1, 136.1, 135.6, 135.3, 130.0 (2C), 129.2, 126.6 (2C), 124.8, 124.7, 123.8, 120.8, 114.5, 109.8, 47.0 (NCH_2), 38.8 (NMe), 27.9 (CH_2), 22.3 (CH_2), 21.6 (ArMe), 14.0 (Me); HPLC: 99.9%, column: Cosmicsil Aura ODS C-18 150 * 4.6 mm 5 µm, mobile phase A: 0.1% TFA in water, mobile phase B: CH_3CN, (gradient) T/B% : 0/10, 20/95, 27/95, 31/10, 35/10; flow rate: 1 mL/min; UV 215.0 nm, retention time 18.8 min; IR (KBr) ν_{max} 2962, 1697, 1529, 1453 cm^{-1}; MS (ES mass): m/z 477.1 (M + 1, 100%).

*4.1.12. 3-{(5-Fluoro-1-tosyl-1H-indol-2-yl)methyl}-5-methyl-7-propyl-3H-pyrazolo[4,3-d][1,2,3]triazin-4(5H)-one (**3f**)*

White solid (74% yield); mp: 140–142 °C; R_f (20% EtOAc/*n*-hexane) 0.24; ^{1}H NMR (400 MHz, $CDCl_3$) δ: 8.03 (dd, J = 8.8, 4.4 Hz, 1H, ArH), 7.79 (d, J = 8.4 Hz, 2H, ArH), 7.27 (d, J = 6.4 Hz, 2H, ArH), 7.02–6.96 (m, 2H, ArH), 6.06 (s, 2H, NCH_2), 6.03 (s, 1H, indole (C-3) H), 4.30 (s, 3H, NCH_3), 3.05 (t, J = 7.6 Hz, 2H, CH_2), 2.36 (s, 3H, $ArCH_3$), 1.97–1.86 (m, 2H, $MeCH_2$), 1.05 (t, J = 7.6 Hz, 3H, CH_3); ^{13}C NMR (100 MHz, $CDCl_3$) δ: 161.0 (C-F J = 239.3 Hz), 150.3 (C═O), 148.7, 145.4, 137.4, 136.2, 135.1, 133.4, 130.3(C-F J = 10.3 Hz), 130.1 (2C), 126.6 (2C), 118.0, 115.7 (C-F J = 9.3 Hz), 112.8 (C-F J = 25.3 Hz), 109.5 (C-F J = 4 Hz), 106.4 (C-F J = 24 Hz), 46.9 (NCH_2), 38.8 (NMe), 27.9 (CH_2), 22.3 (CH_2), 21.6 (ArMe), 14.0 (Me); HPLC: 99.5%, column: Eclips XDB C-18 150 * 4.6 mm 5 µm, mobile phase A: 0.05% TFA in water, mobile phase B: 0.05% TFA in CH_3CN, (gradient) T/B% : 0/10, 5/10, 25/90, 30/90, 31/10, 35/10; flow rate: 1 mL/min; UV 215.0 nm, retention time 25.8 min; MS (ES mass): m/z 495.1 (M + 1, 100%).

*4.1.13. 5-Methyl-3-[{1-(methylsulfonyl)-1H-indol-2-yl}methyl]-7-propyl-3H-pyrazolo[4,3-d][1,2,3]triazin-4(5H)-one (**3g**)*

White solid (76% yield); mp: 78–80 °C; R_f (20% EtOAc/*n*-hexane) 0.24; ^{1}H NMR (400 MHz, $CDCl_3$) δ: 8.01 (d, J = 8.4 Hz, 1H, ArH), 7.45 (d, J = 7.6 Hz, 1H, ArH), 7.37–7.30 (m, 1H, ArH), 7.27–7.23 (m, 1H, ArH), 6.32 (s, 1H, indole (C-3) H), 5.97 (s, 2H, NCH_2), 4.28 (s, 3H, NCH_3), 3.29 (s, 3H, SCH_3), 3.04 (t, J = 7.6 Hz, 2H, CH_2), 1.96–1.85 (m, 2H, $MeCH_2$), 1.04 (t, J = 7.6 Hz, 3H, CH_3); ^{13}C NMR (100 MHz, $CDCl_3$) δ: 150.1 (C═O), 148.6, 136.8, 136.3, 135.4, 129.0, 125.0, 124.7, 123.9, 121.0, 114.0, 110.0, 46.0 (NCH_2), 40.9 (SMe), 38.8 (NMe), 27.9 (CH_2), 22.3 (CH_2), 14.0 (Me); HPLC: 99.9%, column: Eclips XDB C-18 150 * 4.6 mm 5 µm, mobile phase A: 5 mM Ammonium Acetate in water, mobile phase B: CH_3CN, (gradient) T/B% : 0/10, 20/95, 37/95, 40/90, 45/10; flow rate: 1 mL/min; max plot, retention time 16.9 min; IR (KBr) ν_{max} 2960, 1697, 1532, 1405 cm^{-1}; MS (ES mass): m/z 401.1 (M + 1, 100%).

*4.1.14. 3-[{5-Chloro-1-(thiophen-2-ylsulfonyl)-1H-indol-2-yl}methyl]-5-methyl-7-propyl-3H-pyrazolo[4,3-d][1,2,3]triazin-4(5H)-one (**3h**)*

White solid (78% yield); mp: 115–117 °C; R_f (20% EtOAc/*n*-hexane) 0.24; ^{1}H NMR (400 MHz, $CDCl_3$) δ: 8.05 (d, J = 8.8 Hz, 1H, ArH), 7.76 (dd, J = 4.0, 1.6 Hz, 1H, ArH), 7.59 (dd, J = 4.8, 1.2 Hz, 1H, ArH), 7.32–7.26 (m, 2H, ArH), 7.05 (dd, J = 5.2, 4.0 Hz, 1H, ArH), 6.04 (bs, 3H, indole (C-3) H, NCH_2), 4.31 (s, 3H, NCH_3), 3.04 (t, J = 7.6 Hz, 2H, CH_2), 1.97–1.86 (m, 2H, $MeCH_2$), 1.05 (t, J = 7.6 Hz 3H, CH_3); ^{13}C NMR (100 MHz, $CDCl_3$) δ: 150.2 (C═O), 148.7, 137.7, 136.9, 136.1, 135.2, 133.9, 133.2, 130.6, 129.9, 127.8, 125.1, 124.6, 120.5, 115.7, 109.7, 46.8 (NCH_2), 38.8 (NMe), 27.9 (CH_2), 22.3 (CH_2), 14.0 (Me); HPLC: 99.8%, column: Symmetry C-18 75 * 4.6 mm 3.5 µm, mobile phase A: 10 mM Ammonium Formate in water, mobile phase B: CH_3CN (gradient) T/B% : 0/5, 20/90, 30/90, 31/5, 25/20, 30/20; flow rate: 1 mL/min; UV: 225.0 nm, retention time 18.8 min; IR (KBr) ν_{max} 2956, 1705, 1531, 1447 cm^{-1}; MS (ES mass): m/z 503.10 (M + 1, 100%).

*4.1.15. 5-Methyl-7-propyl-3-[{1-(Thiophen-2-ylsulfonyl)-1H-indol-2-yl} methyl]-3H-pyrazolo[4,3-d][1,2,3]triazin-4(5H)-one (**3i**)*

White solid (78% yield); mp: 152–154 °C; R_f (20% EtOAc/*n*-hexane) 0.24; ^{1}H NMR (400 MHz, $CDCl_3$) δ: 8.11 (dd, *J* = 8.4, 0.8 Hz, 1H, ArH), 7.76 (dd, *J* = 4.0, 1.6 Hz, 1H, ArH), 7.54 (dd, *J* = 4.8, 1.6 Hz, 1H, ArH), 7.34–7.29 (m, 2H, ArH), 7.23–7.17 (m, 1H, ArH), 7.01 (dd, *J* = 4.8, 4.0 Hz, 1H, ArH), 6.09 (s, 1H, indole (C-3) H), 6.06 (s, 2H, NCH_2), 4.30 (s, 3H, NCH_3), 3.04 (t, *J* = 7.6 Hz, 2H, CH_2), 1.97–1.86 (m, 2H, $MeCH_2$), 1.05 (t, *J* = 7.6 Hz 3H, CH_3); ^{13}C NMR (100 MHz, $CDCl_3$) δ: 150.2 (C═O), 148.6, 137.9, 136.8, 136.1, 135.3, 133.5, 133.0, 129.4, 127.7, 124.9, 124.6, 124.1, 120.9, 114.6, 110.5, 46.9 (NCH_2), 38.8 (NMe), 27.9 (CH_2), 22.3 (CH_2), 13.9 (Me); HPLC: 99.7%, column: Eclips XDB C-18 150 * 4.6 mm 5 µm, mobile phase A: 0.05% TFA in water, mobile phase B: 0.05% TFA in CH_3CN (gradient) T/B% : 0/10, 5/10, 25/90, 30/90, 31/10, 35/10; flow rate: 1 mL/min; UV 254.0 nm, retention time 24.5 min; IR (KBr) ν_{max} 2956, 1697, 1530, 1452 cm^{-1}; MS (ES mass): *m/z* 469.10 (M + 1, 100%).

*4.1.16. 5-Methyl-3-[{1-(methylsulfonyl)-5-nitro-1H-indol-2-yl}methyl]-7-propyl-3H-pyrazolo[4,3-d][1,2,3]triazin-4(5H)-one (**3j**)*

White solid (80% yield); mp: 175–177 °C; R_f (20% EtOAc/*n*-hexane) 0.2; ^{1}H NMR (400 MHz, DMSO-d_6) δ: 8.47 (d, *J* = 2.0 Hz, 1H, ArH), 8.23 (dd, *J* = 9.2, 2.4 Hz, 1H, ArH), 8.11 (d, *J* = 9.2 Hz, 1H, ArH), 6.71 (s, 1H, indole (C-3) H), 5.94 (s, 2H, NCH_2), 4.20 (s, 3H, NCH_3), 3.70 (s, 3H, SCH_3), 2.97 (t, *J* = 7.6 Hz, 2H, CH_2), 1.93–1.87 (m, 2H, $MeCH_2$), 0.98 (t, *J* = 7.6 Hz, 3H, CH_3); ^{13}C NMR (100 MHz, DMSO-d_6) δ: 149.6 (C═O), 147.0, 143.7, 139.1, 139.0, 135.5, 128.6, 124.6, 119.5, 117.0, 114.4, 109.2, 45.6 (NCH_2), 41.8 (SMe), 38.5 (NMe), 27.2 (CH_2), 21.6 (CH_2), 13.7 (Me); HPLC: 98.7%, column: X Bridge Phenyle 150 * 4.6 mm 3.5 µm, mobile phase A: 0.05% TFA in water, mobile phase B: CH_3CN:water (90:10), (gradient) T/B% : 0/2, 5/2, 20/90, 25/90, 26/2, 30/2; flow rate: 1 mL/min; UV: 250.0 nm, retention time 20.5 min; MS (ES mass): *m/z* 446.1 (M + 1, 100%).

*4.1.17. 5-Methyl-3-{(5-methyl-1-tosyl-1H-indol-2-yl)methyl}-7-propyl-3H-pyrazolo[4,3-d][1,2,3]triazin-4(5H)-one (**3k**)*

White solid (72% yield); mp: 111–113 °C; R_f (20% EtOAc/*n*-hexane) 0.25; ^{1}H NMR (400 MHz, $CDCl_3$) δ: 7.94 (d, *J* = 8.4 Hz, 1H, ArH), 7.79 (d, *J* = 8.4 Hz, 2H, ArH), 7.08 (d, *J* = 8.0 Hz, 2H, ArH), 7.23 (d, *J* = 8.8, 2H, ArH), 6.05 (s, 2H, NCH_2), 6.02 (s, 1H, indole (C-3) H), 4.30 (s, 3H, NCH_3), 3.05 (t, *J* = 7.6 Hz, 2H, CH_2), 2.34 (2 s, 6H, $2ArCH_3$), 1.97–1.86 (m, 2H, $MeCH_2$), 1.04 (t, *J* = 7.6 Hz, 3H, CH_3); ^{13}C NMR (100 MHz, $CDCl_3$) δ: 150.2 (C═O), 148.5, 144.9, 136.1, 135.5, 135.4, 135.3, 133.3, 129.9 (2C), 129.4, 126.6 (2C), 126.1, 124.7, 120.6, 114.1, 109.7, 46.9 (NCH_2), 38.8 (NMe), 27.9 (CH_2), 22.3 (CH_2), 21.5 (ArMe), 21.2 (ArMe), 14.0 (Me); HPLC: 97.4%, column: X Bridge C-18 150*4.6 mm 5 µm, mobile phase A: 5 mM Ammonium acetate in water, mobile phase B: CH_3CN, (gradient) T/B% : 0/5, 20/90, 30/90, 31/5, 35/5; flow rate: 1 mL/min; Max plot, retention time 20.9 min; MS (ES mass): *m/z* 491.1 (M + 1, 100%).

*4.1.18. 3-{(5-Bromo-1-tosyl-1H-indol-2-yl)methyl}benzo[d][1,2,3] triazin-4(3H)-one (**4a**)*

White solid (80% yield); mp: 145–147 °C; R_f (20% EtOAc/*n*-hexane) 0.25; ^{1}H NMR (400 MHz, $CDCl_3$) δ: 8.40 (d, *J* = 8 Hz, 1H, ArH), 8.23 (d, *J* = 8.4 Hz, 1H, ArH), 8.02 (t, *J* = 7.6 Hz, 1H, ArH), 7.98 (d, *J* = 8.8 Hz, 1H, ArH), 7.86 (t, *J* = 7.6 Hz, 1H, ArH), 7.80 (d, *J* = 8.4 Hz, 2H, ArH), 7.43 (d, *J* = 1.2 Hz, 1H, ArH), 7.36(dd, *J* = 8.8 Hz,1.6 Hz, 1H, ArH), 7.27 (d, *J* = 8.4 Hz, 2H, ArH), 6.10 (s, 2H, NCH_2), 6.07 (s, 1H, indole (C-3) H), 2.36 (s, 3H, $ArCH_3$); ^{13}C NMR (100 MHz, $CDCl_3$) δ: 155.3 (C═O), 145.5, 144.3, 136.8, 135.7, 135.3, 135.0, 132.8, 130.9, 130.1 (2C), 128.6, 127.6, 126.6 (2C), 125.3, 123.4, 119.8, 117.1, 115.8, 108.9, 47.7 (NCH_2), 21.6 (ArMe); HPLC: 99.2%, column: X Bridge C-18 150 * 4.6 mm 5 µm, mobile phase A: 0.1% TFA in water, mobile phase B: CH_3CN, (gradient) T/B% : 0/10, 3/10, 12/95, 23/95, 25/10, 30/10; flow rate: 1 mL/min; UV 225.0 nm, retention time 18.6 min; IR (KBr) ν_{max} 2958, 1708, 1533, 1448 cm^{-1}; MS (ES mass): *m/z* 510.9 (M + 2, 100%), 508.9 (M^+, 98%).

*4.1.19. 3-[{5-Chloro-1-(methylsulfonyl)-1H-indol-2-yl}methyl]benzo[d][1,2,3]triazin-4(3H)-one (**4b**)*

White solid (78% yield); mp: 154–156 °C; R_f (20% EtOAc/*n*-hexane) 0.25; ^{1}H NMR (400 MHz, $CDCl_3$) δ: 8.36 (d, *J* = 8 Hz, 1H, ArH), 8.23 (d, *J* = 8 Hz, 1H, ArH), 8.02 (t, *J* = 7.6 Hz, 1H, ArH), 7.95 (d, *J* = 8.8 Hz, 1H, ArH), 7.86 (t, *J* = 7.6 Hz, 1H, ArH), 7.41 (s, 1H, ArH), 7.29 (d, *J* = 9.2 Hz, 1H, ArH), 6.32 (s, 1H, indole (C-3) H), 6.00 (s, 2H, NCH_2), 3.33 (s, 3H, SCH_3); ^{13}C NMR (100 MHz, $CDCl_3$) δ: 155.3 (C═O), 144.4, 136.8, 135.3, 135.1, 132.9, 130.2, 129.7, 128.6, 125.2, 125.2, 120.5, 119.8, 115.0, 109.2, 46.8 (NCH_2), 41.2 (SMe); HPLC: 99.1%, column: Cosmicsil Aura ODS 150 * 4.6 mm 5 µm, mobile phase A: 5 mM Ammonium Acetate in water, mobile phase B: CH_3CN, (gradient) T/B%: 0/10, 20/90, 28/90, 30/10, 35/10; flow rate: 1 mL/min; UV 225.0 nm, retention time 17.9 min; IR (KBr) ν_{max} 1683, 1585, 1448, 1361 cm^{-1}; MS (ES mass): *m/z* 389.1 (M + 1, 100%).

*4.1.20. 3-[{1-(Phenylsulfonyl)-1H-indol-2-yl}methyl]benzo[d][1,2,3] triazin-4(3H)-one (**4c**)*

White solid (74% yield); mp: 112–114 °C; R_f (20% EtOAc/*n*-hexane) 0.25; ^{1}H NMR (400 MHz, $CDCl_3$) δ: 8.40 (m, *J* = 8.8 Hz, 1H, ArH), 8.23 (d, *J* = 8.4 Hz, 1H, ArH), 8.08 (d, *J* = 8 Hz, 1H, ArH), 8.04–7.99 (m, 1H, ArH), 7.94(d, *J* = 8 Hz, 2H, ArH), 7.88–7.83 (m, 1H, ArH), 7.55 (t, *J* = 7.6 Hz, 1H, ArH), 7.48 (t, *J* = 7.6 Hz, 2H, ArH), 7.33–7.27 (m, 2H, ArH), 7.17 (t, *J* = 7.2 Hz, 1H, ArH), 6.16 (s, 1H, indole (C-3) H), 6.12 (s, 2H, NCH_2); ^{13}C NMR (100 MHz, $CDCl_3$) δ: 155.3 (C═O), 144.3, 138.2, 137.0, 135.4, 135.2, 134.0, 132.7, 129.4 (2C), 129.2, 128.6, 126.6 (2C), 125.3, 124.8, 123.8, 120.8, 119.8, 114.4, 110.1, 47.8 (NCH_2); HPLC: 93.7%, column: Eclips plus 250 * 4.6 mm 5 µm, mobile phase A: 0.1% TFA in water, mobile phase B: CH_3CN, (gradient) T/B% : 0/5, 20/90, 30/90, 3/5, 35/5; flow rate: 1 mL/min; UV 215.0 nm, retention time 20.5 min; MS (ES mass): *m/z* 417.1 (M + 1, 100%).

*4.1.21. 3-{(5-Chloro-1-tosyl-1H-indol-2-yl)methyl}benzo[d][1,2,3] triazin-4(3H)-one (**4d**)*

White solid (81% yield); mp: 154–156 °C; R_f (20% EtOAc/*n*-hexane) 0.25; ^{1}H NMR (400 MHz, $CDCl_3$) δ: 8.39 (d, *J* = 8.0 Hz, 1H, ArH), 8.22 (d, *J* = 8.0 Hz, 1H, ArH), 8.03–7.99 (m, 2H, ArH), 7.85 (t, *J* = 7.6 Hz, 1H, ArH), 7.80 (t, *J* = 8.4 Hz, 2H, ArH), 7.28–7.25 (m, 3H, ArH), 7.22 (dd, *J* = 8.8, 2.0 Hz, 1H, ArH), 6.09 (s, 2H, NCH_2), 6.08 (s, 1H, indole (C-3) H), 2.34 (s, 3H, $ArCH_3$); ^{13}C NMR (100 MHz, $CDCl_3$) δ: 155.3 (C═O), 145.5, 144.3, 136.9, 135.3, 135.2, 135.0, 132.8, 130.4, 130.1 (2C), 129.5, 128.6, 126.6 (2C), 125.3, 124.9, 120.3, 119.8, 115.5, 109.0, 47.7 (NCH_2), 21.6 (ArMe); HPLC: 99.9%, column: Symmetry C-18 4.6 * 75 mm 3.5 µm, mobile phase A: 10 mM Ammonium Formate in water, mobile phase B: CH_3CN, (gradient) T/B% : 0/10, 3/10, 15/95, 20/95, 21/10, 25/10; flow rate: 1 mL/min; UV 225.0 nm, retention time 14.8 min; IR (KBr) ν_{max} 3088, 1672, 1596, 1442 cm^{-1}; MS (ES mass): *m/z* 465.0 (M + 1, 50%), 318.0 (M−146, 100%).

*4.1.22. 3-{(1-Tosyl-1H-indol-2-yl)methyl}benzo[d][1,2,3]triazin-4(3H)-one (**4e**)*

White solid (77% yield); mp: 173–175 °C; R_f (20% EtOAc/*n*-hexane) 0.25; ^{1}H NMR (400 MHz, $CDCl_3$) δ: 8.40 (d, *J* = 7.6 Hz, 1H, ArH), 8.22 (d, *J* = 8.4 Hz, 1H, ArH), 8.09 (d, *J* = 8.40 Hz, 1H, ArH), 8.00 (t, *J* = 7.6 Hz, 1H, ArH), 7.89–7.79 (m, 3H, ArH), 7.34–7.22 (m, 4H, ArH), 7.16 (t, *J* = 7.2 Hz, 1H, ArH), 6.14 (s, 1H, indole (C-3) H), 6.12 (s, 2H, NCH_2), 2.34 (s, 3H, $ArCH_3$); ^{13}C NMR (100 MHz, $CDCl_3$) δ: 155.3 (C═O), 145.1, 144.3, 137.0, 135.4, 135.3, 135.1, 132.643, 130.0 (2C), 129.2, 128.5, 126.6 (2C), 125.3, 124.7, 123.7, 120.7, 119.8, 114.4, 109.8, 47.9 (NCH_2), 21.6 (ArMe); HPLC: 99.9%, column: X-Bridge C18 150 * 4.6 mm 5 µm, mobile phase A: 0.1% TFA in water, mobile phase B: CH_3CN, (gradient) T/B% : 0/10, 20/95, 31/10, 35/10; flow rate: 1 mL/min; UV 220.0 nm, retention time 17.0 min; IR (KBr) ν_{max} 3084,

1679, 1595, 1450 cm^{-1}; MS (ES mass): *m/z* 431.1 (M + 1, 25%), 284.0 (M − 146, 100%).

4.1.23. 3-{(5-Fluoro-1-tosyl-1H-indol-2-yl)methyl}benzo[d][1,2,3]triazin-4(3H)-one (4f)

White solid (71% yield); mp: 176–178 °C; R_f (20% EtOAc/*n*-hexane) 0.25; ^{1}H NMR (400 MHz, $CDCl_3$) δ: 8.40 (d, *J* = 7.6 Hz, 1H, ArH), 8.23 (d, *J* = 8.4 Hz, 1H, ArH), 8.08–7.98 (m, 2H, ArH), 7.86 (t, *J* = 7.2 Hz, 1H, ArH), 7.81 (d, *J* = 7.6 Hz, 2H, ArH), 7.27 (d, *J* = 7.2 Hz, 2H, ArH), 7.02–6.92 (m, 2H, ArH), 6.10 (bs, 3H, NCH_2, indole (C-3) H), 2.36 (s, 3H, $ArCH_3$); ^{13}C NMR (100 MHz, $CDCl_3$) δ: 160.9 (C-F *J* = 245.6 Hz), 155.3 (C═O), 145.4, 144.291, 135.3, 135.2, 135.0, 132.8, 132.8, 130.1 (C-F *J* = 11.6 Hz), 130.1 (2C), 129.7, 128.6, 126.6 (2C), 125.3, 115.6 (C-F *J* = 10.7 Hz), 112.7 (C-F *J* = 25.6 Hz), 109.5 (C-F *J* = 2.8 Hz), 106.4 (C-F *J* = 24.7 Hz), 47.9 (NCH_2), 21.6 (ArMe); HPLC: 98.1%, column: Cosmicsil Aura ODS C-18 150*4.6 mm 5 µm, mobile phase A: 5 mM Ammonium acetate in water, mobile phase B: CH_3CN, (gradient) T/B% : 0/5, 20/90, 25/90, 26/3, 30/5; flow rate: 1 mL/min; UV 220.0 nm, retention time 19.3 min; IR (KBr) ν_{max} 3102, 1681, 1595, 1467 cm^{-1}; MS (ES mass): *m/z* 449.1 (M + 1, 100%).

4.1.24. 3-{(1-(Methylsulfonyl)-1H-indol-2-yl)methyl}benzo[d][1,2,3]triazin-4(3H)-one (4g)

White solid (80% yield); mp: 134–136 °C; R_f (20% EtOAc/*n*-hexane) 0.25; ^{1}H NMR (400 MHz, $CDCl_3$) δ: 8.36 (d, *J* = 8.0 Hz, 1H, ArH), 8.21 (d, *J* = 8.0 Hz, 1H, ArH), 8.05–7.97 (m, 2H, ArH), 7.84 (t, *J* = 7.6 Hz, 1H, ArH), 7.44 (d, *J* = 7.6 Hz, 1H, ArH), 7.34 (t, *J* = 7.6 Hz, 1H, ArH), 7.25 (t, *J* = 7.2 Hz, 1H, ArH), 6.38 (s, 1H, indole (C-3) H), 6.01 (s, 2H, NCH_2), 3.31 (s, 3H, SCH_3); ^{13}C NMR (100 MHz, $CDCl_3$) δ: 155.3 (C═O), 144.4, 136.8, 135.3, 135.2, 132.8, 129.1, 128.6, 125.2, 125.1, 123.9, 121.0, 119.9, 114.0, 110.1, 47.0 (NCH_2), 41.0 (SMe); HPLC: 99.2%, column: Eclips XDB C-18 150 * 4.6 mm 5 µm, mobile phase A: 0.05% TFA in water, mobile phase B: 0.05% TFA in CH_3CN, (gradient) T/B% : 0/10, 5/10, 25/90, 30/90, 31/10, 35/10; flow rate: 1 mL/min; UV 220.0 nm, retention time 20.0 min; IR (KBr) ν_{max} 3029, 1683, 1448, 1405 cm-1; MS (ES mass): *m/z* 355.1 (M + 1, 20%), 208.1 (M − 146, 100%).

4.1.25. 3-{(5-Chloro-1-(thiophen-2-ylsulfonyl)-1H-indol-2-yl}methyl)benzo[d][1,2,3]triazin-4(3H)-one (4h)

White solid (80% yield); mp: 213–215 °C; R_f (20% EtOAc/*n*-hexane) 0.25; ^{1}H NMR (400 MHz, $CDCl_3$) δ: 8.37 (dd, *J* = 8.0, 0.8 Hz, 1H, ArH), 8.20 (d, *J* = 8.0 Hz, 1H, ArH), 8.05–7.96 (m, 2H, ArH), 7.83 (t, *J* = 8.0 Hz, 1H, ArH), 7.76 (dd, *J* = 8.0, 1.2 Hz, 1H, ArH), 7.57 (dd, *J* = 4.8, 1.2 Hz, 1H, ArH), 7.25 (d, *J* = 9.6 Hz, 2H, ArH), 7.03 (dd, *J* = 4.8, 4.0 Hz, 1H, ArH), 6.07 (s, 1H, indole (C-3) H), 6.06 (s, 2H, NCH_2); ^{13}C NMR (100 MHz, $CDCl_3$) δ: 155.3 (C═O), 144.3, 137.7, 136.8, 135.3, 135.2, 133.9, 133.3, 132.8, 130.6, 129.9, 128.7, 127.9, 125.3, 125.1, 120.5, 119.8, 115.7, 109.8, 47.7 (NCH_2); HPLC: 99.9%, column: Symmetry C-18 75 * 4.6 mm 3.5 µm, mobile phase A: 10 mM Ammonium Formate in water, mobile phase B: CH_3CN, (gradient) T/B % : 0/5, 20/90, 30/90, 31/5, 35/5; flow rate: 1 mL/min; UV 225.0 nm, retention time 17.0 min; IR (KBr) ν_{max} 3099, 1686, 1585, 1446 cm^{-1}; MS (ES mass): *m/z* 457.0 (M + 1, 69%), 309.9 (M − 146, 100%).

4.1.26. 3-{(1-(Thiophen-2-ylsulfonyl)-1H-indol-2-yl}methyl)benzo[d][1,2,3]triazin-4(3H)-one (4i)

White solid (78% yield); mp: 131–133 °C; R_f (20% EtOAc/*n*-hexane) 0.25; ^{1}H NMR (400 MHz, $CDCl_3$) δ: 8.40 (dd, *J* = 8.0, 0.8 Hz, 1H, ArH), 8.23 (d, *J* = 8.0 Hz, 1H, ArH), 8.12 (d, *J* = 8.8 Hz, 1H, ArH), 8.05–7.97 (m, 1H, ArH), 7.89–7.81 (m, 1H, ArH), 7.78 (dd, *J* = 3.6, 1.2 Hz, 1H, ArH), 7.55 (dd, *J* = 4.8, 1.2 Hz, 1H, ArH), 7.31 (t, *J* = 7.6 Hz, 2H, ArH), 7.20 (t, *J* = 7.6 Hz, 1H, ArH), 7.02 (dd, *J* = 4.8, 4.0 Hz, 1H, ArH), 6.15 (s, 1H, indole (C-3) H), 6.08 (s, 2H, NCH_2); ^{13}C NMR (100 MHz, $CDCl_3$) δ: 155.3 (C═O), 144.3, 138.0, 136.8, 135.2, 135.2, 133.6, 133.0, 132.7, 129.4, 128.6, 127.7, 125.3, 124.9, 124.1, 120.9, 119.8, 114.6, 110.6, 47.8 (NCH_2); HPLC: 99.8%, column: Eclips XDB C-18 150*4.6 mm 5 µm, mobile phase A: 0.05% TFA in water, mobile phase B: 0.05% TFA in CH_3CN, (gradient) T/B% : 0/10, 5/10, 25/90, 30/90, 31/10, 35/10; flow rate: 1 mL/min; UV 254.0 nm, retention time 22.3 min; IR (KBr) ν_{max} 3090, 1684, 1606, 1451 cm^{-1}; MS (ES mass): *m/z* 423.0 (M + 1, 100%).

4.1.27. 3-[{5-Fluoro-1-(methylsulfonyl)-1H-indol-2-yl}methyl]benzo[d][1,2,3]triazin-4(3H)-one (4j)

White solid (72% yield); mp: 154–156 °C; R_f (20% EtOAc/*n*-hexane) 0.25; ^{1}H NMR (400 MHz, $CDCl_3$) δ: 8.36 (d, *J* = 8 Hz, 1H, ArH), 8.23 (d, *J* = 8.4 Hz, 1H, ArH), 8.00 (m, 2H, ArH), 7.86 (t, *J* = 7.6 Hz, 1H, ArH), 7.07 (m, 2H, ArH), 6.33 (s, 1H, indole (C-3) H), 6.00 (s, 2H, NCH_2), 3.32 (s, 3H, SCH_3); ^{13}C NMR (100 MHz, $CDCl_3$) δ: 160.9 (C-F *J* = 239.6 Hz), 155.3 (C═O), 144. 4, 137.0, 135.3, 133.0, 132.8, 130.1(C-F *J* = 10.2 Hz), 128.6, 125.2, 119.8, 115.2 (C-F *J* = 9.2 Hz), 113.1 (C-F *J* = 25.1 Hz), 109.6 (C-F *J* = 4 Hz), 106.6 (C-F *J* = 24 Hz), 46.9 (NCH_2), 41.0 (SMe); HPLC: 97.4%, column: Eclipse plus C-18 250 * 4.6 mm 5 µm, mobile phase A: 0.1% TFA in water, mobile phase B: CH_3CN, (gradient) T/B% : 0/5, 20/90, 28/90, 30/5, 35/5, flow rate: 1 mL/min; UV 225.0 nm, retention time 18.3 min; MS (ES mass): *m/z* 373.1 (M + 1, 100%).

4.1.28. 3-{(5,7-Dimethyl-1-(methylsulfonyl)-1H-indol-2-yl)methyl}benzo[d][1,2,3]triazin-4(3H)-one (4k)

White solid (68% yield); mp: 159–161 °C; R_f (20% EtOAc/*n*-hexane) 0.24; ^{1}H NMR (400 MHz, $CDCl_3$) δ: 8.35 (d, *J* = 7.6 Hz, 1H, ArH), 8.19 (d, *J* = 8.0 Hz, 1H, ArH), 7.98 (t, *J* = 7.6 Hz, 1H, ArH), 7.83 (t, *J* = 7.6 Hz, 1H, ArH), 7.26 (s, 1H, ArH), 6.94 (s, 1H, ArH), 6.43 (s, 1H, indole (C-3) H), 5.97 (s, 2H, NCH_2), 3.20 (s, 3H, SCH_3), 2.64 (s, 3H, $ArCH_3$), 2.32 (s, 3H, $ArCH_3$); ^{13}C NMR (100 MHz, $CDCl_3$) δ: 155.2 (C═O), 144.3, 138.4, 137.1, 135.1, 134.7, 132.7, 132.2, 130.5, 128.5, 127.1, 125.2, 119.9, 119.0, 114.8, 48.0 (NCH_2), 40.0 (SMe), 21.8 (ArMe), 20.8 (ArMe); HPLC: 99.4%, column: Eclips XDB C18 ODS 150 * 4.6 mm 5 µm, mobile phase A: 0.05% TFA in water, mobile phase B: 0.05% TFA in CH_3CN, (gradient) T/B% : 0/10, 5/10, 25/90, 30/90, 31/10, 35/10; flow rate: 1 mL/min; UV 225.0 nm, retention time 22.1 min; IR (KBr) ν_{max} 3111, 1685, 1461, 1444 cm^{-1}; MS (ES mass): *m/z* 383.1 (M + 1, 100%).

4.1.29. 3-{(5,7-Dimethyl-1-(phenylsulfonyl)-1H-indol-2-yl)methyl}benzo[d][1,2,3]triazin-4(3H)-one (4l)

White solid (66% yield); mp: 136–138 °C; R_f (20% EtOAc/*n*-hexane) 0.24; ^{1}H NMR (400 MHz, $CDCl_3$) δ: 8.37 (dd, *J* = 8.0, 0.8 Hz, 1H, ArH), 8.20 (dd, *J* = 8.0, 0.4 Hz, 1H, ArH), 8.01–7.94 (m, 1H, ArH), 7.86–7.79 (m, 1H, ArH), 7.71–7.65 (m, 2H, ArH), 7.54–7.47 (m, 1H, ArH), 7.41–7.35 (m, 2H, ArH), 6.88 (s, 1H, ArH), 6.81 (s, 1H, ArH), 6.12 (s, 1H, indole (C-3) H), 6.02 (s, 2H, NCH_2), 2.60 (s, 3H, $ArCH_3$), 2.23 (s, 3H, $ArCH_3$); ^{13}C NMR (100 MHz, $CDCl_3$) δ: 155.3 (C═O), 155.25, 144.3, 139.0, 137.2, 135.1, 134.7, 133.5, 132.8, 132.6, 130.4, 128.8 (2C), 128.5, 127.7, 126.6 (2C), 125.3, 119.9, 118.7, 115.0, 48.9 (NCH_2), 21.8 (ArMe), 20.8 (ArMe); HPLC: 99.9%, column: X-Bridge C18 150 * 4.6 mm 5 µm, mobile phase A: 0.1% TFA in water, mobile phase B: CH_3CN, (gradient) T/B% : 0/10, 20/95, 31/10, 35/10; flow rate: 1 mL/min; UV 220.0 nm, retention time 17.8 min; IR (KBr) ν_{max} 3006, 1688, 1607, 1443 cm^{-1}; MS (ES mass): *m/z* 445.1 (M + 1, 34%), 298.0 (M − 146, 100%).

4.1.30. 6-Bromo-3-{(5-chloro-1-tosyl-1H-indol-2-yl)methyl}benzo[d][1,2,3]triazin-4(3H)-one (4m)

White solid (79% yield); mp: 169–171 °C; R_f (20% EtOAc/*n*-hexane) 0.3; ^{1}H NMR (400 MHz, $CDCl_3$) δ: 8.54–8.51 (m, 1H, ArH), 8.12–8.05 (m, 2H, ArH), 8.01 (d, *J* = 8.8 Hz, 1H, ArH), 7.79 (d, *J* = 8.4 Hz, 2H, ArH), 7.31–7.27 (m, 2H, ArH), 7.26–7.21 (m, 2H, ArH), 6.09 (s, 1H, indole (C-3) H), 6.07 (s, 2H, NCH_2), 2.36 (s, 3H, $ArCH_3$); ^{13}C NMR (100 MHz, $CDCl_3$) δ: 154.1 (C═O), 145.5, 142.9, 138.6, 136.6, 135.4,

135.1, 130.3, 130.2, 130.1 (2C), 129.6, 128.1, 127.5, 126.6 (2C), 125.1, 121.0, 120.4, 115.6, 109.3, 47.8 (NCH_2), 21.6 (ArMe); HPLC: 99.7%, column: X-Bridge C-18 4.6 mm 5 μm, mobile phase A: 5 mM Ammonium acetate in water, mobile phase B: CH_3CN, (gradient) T/B% : 0/10, 23/90, 30/90, 31/90, 35/10; flow rate: 1 mL/min; Max plot, retention time 23.4 min; MS (ES mass): *m/z* 544.9 (M + 2, 40%), 317.9 (M − 227, 100%).

5. Docking study

5.1. Materials and methods

It is known that the secreted chorismate mutase of *Mtb* which is encoded by Rv1885c gene is the major contributor in shikimate pathway commonly occurred in cytoplasm of bacteria [17]. For our study we searched for the available crystal structure of secreted *Mtb*CM and found four structures in Protein Data Bank (PDB) [18], represented as follows

PDB ID	Resolution (Å)	Co-crystal ligand(s)
2AO2	2.07	SO4 and Trp[a]
2F6L	1.70	Not available
2FP1	1.55	PB
2FP2	1.64	TSA[b]

[a]Trp represents tryptophan.

[b]TSA represents transition state analogue i.e. 8-hydroxy-2-oxa-bicyclo[3.3.1]non-6-ene-3,5-dicarboxylic acid.

Among these four crystal structures, we have chosen 2FP2 (PDB ID), because of its low resolution value and presence of substrate molecule as co-crystal structure.

All ligand structures were built in MarvinSketch [19]. Protein (2FP2) as well as all ligands was prepared (means optimization, charge calculation, deletion of co-crystal ligand, and addition of hydrogen etc.) using AutoDock tool [20]. All ligands were docked at the interface site of *Mtb*CM (which is homodimer) using reliable open-source tool AutoDock Vina [21]. The grid map was made up of 20X20X20 points using AutoGrid with 0.54, 3.92, and 42.25 as center_X, center_Y, and center_Z respectively. To search all possible conformation of ligands thoroughly, exhaustiveness value of 20 were used. The Maestro visualizer (Schrodinger, LLC) and UCSF Chimera [22] was used to analyze the interactions of studied ligands at defined binding site.

The molecular docking was performed to evaluate precise binding of test molecules to the interface site of *Mtb*CM. The binding energy of best pose of each ligand is presented in Chart 1. To check the reproducibility of docking result, the docking of each individual ligand was performed at least ten times and maximum difference found was ± 0.2. The validation of docking protocol was done by re-docking the co-crystal ligand (TSA) and calculating RMSD difference between co-crystal one and docked one in PyMOL [23], maximum RMSD was 1.713 (< 2) which confirmed the authenticity of current docking protocol.

6. Pharmacology

6.1. In vitro assay for CM inhibition

6.1.1. Enzyme and reagents

Mycobacterium tuberculosis chorismate mutase (*Mtb*CM) gene was PCR amplified and cloned into expression vector pET22b. *Mtb*CM was purified from over expressed culture of BL21 (DE3) harboring pET22b/*Mtb*CM by Ni-NTA affinity chromatography. The substrate chorismic acid was obtained from Sigma (SIGMA cat # 1701).

6.1.2. CM enzymatic assay

Activity of chorismate mutase enzyme was based on the direct observation of conversion of chorismate to prephenate spectrophotometrically at OD_{274}. The reaction volume of the assay was maintained at 100 μl. The substrate chorismic acid (2 mM) was pre incubated at 37 °C for 5 min in the buffer containing 50 mM Tris-HCl (pH 7.5), 0.5 mM EDTA, 0.1 mg/ml bovine serum albumin, and 10 mM β-Mercaptoethanol. The reaction was started by adding 180 pmol of CM enzyme to the pre-warmed chorismic acid solution. Inhibitory screening of the test compounds against CM activity was measured at 30 μM (10 nM to 30 μM for concentration dependent study) concentration of the effectors. The reaction was allowed to proceed at 37 °C and was terminated after 5 min with 100 μl of 1 N HCl and absorbance was read at 274 nm. Alternatively, the reaction was allowed to proceed for further 10 min and was then terminated with 180 μM of 2.5 N NaOH and absorbance was measured at 320 nm. A blank with no enzyme for every reaction was kept as a control to account for the non enzymatic conversion of chorismate to prephenate. The % of enzyme inhibition caused by the test compound was calculated by the following formula:

$$\% \text{ inhibition} = 100 - \text{residual activity of CM}$$

$$\text{Residual activity of CM} = [A_{274}\{S + (E' + C)\} - A_{274}(S + C)]/[A_{274}(S + E) - A_{274}(S)]$$

S = absorbance of the substrate (chorismic acid) at 274 nm; E′ = absorbance of the enzyme (CM) at 274 nm with compound; E = absorbance of the enzyme (CM) at 274 nm without compound; C = test compound; A_{274} indicates absorbance at 274 nm (this is replaced by A_{320} for absorbance at 320 nm).

6.2. MTT assay

20,000–25,000 cells per well were seeded in a 96-well plate and incubated with the compound at different concentrations for 24 h. After treatment, MTT [3-(4,5-dimethylthiazol-2-yl)-2,5-diphenyltetrazolium bromide] reagent was added to a final concentration of 0.25 mg/mL and incubated at 37 °C for 2 h. After 2 h, media was removed completely, and the intracellular purple formazan crystals were dissolved in 100 μl of DMSO. The absorbance of this solution was measured at 570 nm. Each concentration of compound was performed in triplicate and the relative cell viability was expressed as a percentage relative to the untreated control cells.

7. Computational ADME prediction

7.1. Software and methods

The ADME predictions were performed by using the SwissADME web-tool [15], where the molecules were drawn using Marvin JS (version 16.4.18, 2016) and converted into SMILES by JChem Web Services (version 14.9.29, 2013). Then the 3D conformations were generated through the StringMolExport function. All descriptors and important molecular parameters of physicochemical properties were computed by OpenBable API (version 2.3.0, 2012). The predictive models were mostly generated by Quantitative Structure-Property Relationship (QSPR) methods along with some other robust models. As the SwissADME is a web-based tool, all these process are done in an automated manner.

Acknowledgements

GSR thanks DST, India for a INSPIRE fellowship (IF160590). Authors thank the Management of DRILS, Hyderabad, India and Manipal University, Manipal, India for encouragement and support and DBT, New Delhi, India for financial assistance (Grant No. BT/PR12817/COE/34/23/2015).

Appendix A. Supplementary material

Supplementary data to this article can be found online at https://doi.org/10.1016/j.bioorg.2019.103155.

References

[1] Tuberculosis: Key Fact; WHO. https://www.who.int/en/news-room/fact-sheets/detail/tuberculosis. Accessed on April 14, 2019.

[2] R.M. Houben, P.J. Dodd, The global burden of latent tuberculosis infection: a re-estimation using mathematical modelling, PLoS Med. 13 (2016) e1002152.

[3] E. Haslam, Shikimic Acid: Metabolism and Metabolites, Wiley, New York, 1993.

[4] For a review, see: M. Khanapur, M. Alvala, M. Prabhakar, K.S. Kumar, R.K. Edwin, P.S.V.K.S. Saranya, R.K. Patel, G. Bulusu, P. Misra, M. Pal, Mycobacterium tuberculosis chorismate mutase: a potential target for TB, Bioorg. Med. Chem. 25 (2017) 1725–1736.

[5] End to killer TB? Scientists identify an enzyme that may hold clue; https://researchmatters.in/article/end-killer-tb-scientists-identify-enzymemay-hold-clue.

[6] K.S. Kumar, R. Adepu, S. Sandra, D. Rambabu, G.R. Krishna, C.M. Reddy, P. Misra, M. Pal, Cu-mediated N-arylation of 1, 2, 3-triazin-4-ones: synthesis of fused triazinone derivatives as potential inhibitors of chorismate mutase, Bioorg. Med. Chem. Lett. 22 (2012) 1146–1150.

[7] A. Nakhi, B. Prasad, U. Reddy, R.M. Rao, S. Sandra, R. Kapavarapu, D. Rambabu, G.R. Krishna, C.M. Reddy, K. Ravada, P. Misra, J. Iqbal, M. Pal, A new route to indoles via in situ desilylation–Sonogashira strategy: identification of novel small molecules as potential anti-tuberculosis agents, Med. Chem. Commun. 2 (2011) 1006–1010.

[8] H. Agrawal, A. Kumar, N.C. Bal, M.I. Siddiqi, A. Arora, Ligand based virtual screening and biological evaluation of inhibitors of chorismate mutase (Rv1885c) from Mycobacterium tuberculosis H37Rv, Bioorg. Med. Chem. Lett. 17 (2007) 3053–3058.

[9] (a) S. Cacchi, G. Fabrizi, L.M. Parisi, 2-aryl and 2-heteroaryl indoles from 1-alkynes and o-iodotrifluoroacetanilide through a domino copper-catalyzed coupling − cyclization process, Org. Lett. 5 (2003) 3843–3846;
(b) S. Cacchi, G. Fabrizi, L.M. Parisi, R. Bernini, 2-Aryl and 2-heteroaryl pyrrolo [2, 3-b] quinoxalines via copper-catalyzed reaction of 1-alkynes with 2-bromo-3-trifluoroacetamidoquinoxaline, Synlett 287–290 (2004);
(c) G.A. Slough, V. Krchnak, P. Helquist, S.M. Canham, Synthesis of readily cleavable immobilized 1, 10-phenanthroline resins, Org. Lett. 6 (2004) 2909–2912;
(d) F. Liu, D. Ma, Assembly of conjugated enynes and substituted indoles via CuI/amino acid-catalyzed coupling of 1-alkynes with vinyl iodides and 2-bromotrifluoroacetanilides, J. Org. Chem. 72 (2007) 4844–4850.

[10] (a) M. Pal, V. Subramanian, V.R. Batchu, I. Dager, Synthesis of 2-substituted indoles via Pd/C-catalyzed reaction in water, Synlett 1965–1969 (2004);
(b) M. Layek, U. Lakshmi, D. Kalita, D.K. Barange, A. Islam, K. Mukkanti, M. Pal, Pd/C-mediated synthesis of indoles in water, Beilstein J. Org. Chem 5 (2009) 46, https://doi.org/10.3762/bjoc.5.46;
(c) R.M. Rao, U. Reddy, A. Nakhi, N. Mulakayala, M. Alvala, M.K. Arunasree, R.R. Poondra, J. Iqbal, M. Pal, Sequential coupling/desilylation–coupling/cyclization in a single pot under Pd/C–Cu catalysis: synthesis of 2-(hetero) aryl indoles, Org. Biomol. Chem. 9 (2011) 3808–3816;
(d) B. Prasad, R. Adepu, S. Sandra, D. Rambabu, G.R. Krishna, C.M. Reddy, G.S. Deora, P. Misra, M. Pal, AlCl3 mediated unexpected migration of sulfonyl groups: regioselective synthesis of 7-sulfonyl indoles of potential pharmacological interest, Chem. Commun. 48 (2012) 10434–10436.

[11] H. Oskooie, M. Heravi, F. Behbahani, A facile, mild and efficient one-pot synthesis of 2-substituted indole derivatives catalyzed by $Pd(PPh_3)_2Cl_2$, Molecules 12 (2007) 1438–1446.

[12] (a) S. Cacchi, G. Fabrizi, Synthesis and functionalization of indoles through palladium-catalyzed reactions, Chem. Rev. 105 (2005) 2873–2920 For selected reviews, see:;
(b) G. Zeni, R.C. Larock, Synthesis of heterocycles via palladium π-olefin and π-alkyne chemistry, Chem. Rev. 104 (2004) 2285–2310;
(c) D.A. Horton, G.T. Bourne, M.L. Smythe, The combinatorial synthesis of bicyclic privileged structures or privileged substructures, Chem. Rev. 103 (2003) 893–930;
(d) H.J. Knolker, K.R. Reddy, Isolation and synthesis of biologically active carbazole alkaloids, Chem. Rev. 102 (2002) 4303–4428;
(e) R. Vicente, Recent advances in indole synthesis: new routes for a classical target, Org. Biomol. Chem. 9 (2011) 6469–6480 and references cited therein.

[13] (a) K. Sonogashira, Y. Tohda, N. Hagihara, A convenient synthesis of acetylenes: catalytic substitutions of acetylenic hydrogen with bromoalkenes, iodoarenes and bromopyridines, Tetrahedron Lett. 16 (1975) 4467–4470;
(b) R. Chinchilla, C. Nájera, Recent advances in Sonogashira reactions, Chem. Soc. Rev. 40 (2011) 5084–5121.

[14] (a) S.K. Kim, S.K. Reddy, B.C. Nelson, G.B. Vasquez, A. Davis, A.J. Howard, S. Patterson, G.L. Gilliland, J.E. Ladner, P.T. Reddy, Biochemical and structural characterization of the secreted chorismate mutase (Rv1885c) from Mycobacterium tuberculosis H37Rv: an* AroQ enzyme not regulated by the aromatic amino acids, J. Bacteriol. 188 (2006) 8638–8648;
(b) S. Sasso, C. Ramakrishnan, M. Gamper, D. Hilvert, P. Kast, Characterization of the secreted chorismate mutase from the pathogen Mycobacterium tuberculosis, FEBS J. 272 (2005) 375–389.

[15] A. Daina, O. Michielin, V. Zoete, SwissADME: a free web tool to evaluate pharmacokinetics, drug-likeness and medicinal chemistry friendliness of small molecules, Sci. Rep. 7 (2017) 42717.

[16] (a) Y. Chang, J. Zhang, X. Chen, Z. Li, X. Xu, Synthesis and nematicidal activities of 1,2,3-benzotriazin-4-one derivatives containing thiourea and acylthiourea against meloidogyne incognita, Bioorg. Med. Chem. Lett. 27 (2017) 2641–2644;
(b) G. Wang, X. Chen, Y. Deng, Z. Li, X. Xu, Synthesis and nematicidal activities of 1,2,3-benzotriazin-4-one derivatives against meloidogyne incognita, J. Agric. Food Chem. 63 (2015) 6883–6889;
(c) T.S. Ibrahim, A.A. Rashad, Z.K. Abdel-Samii, S.A. El-Feky, M.K. Abdel-Hamid, W. Barakat, Synthesis, molecular modelling and anti-inflammatory screening of new 1,2,3-benzotriazinone derivatives, Med. Chem. Res. 21 (2012) 4369–4380;
(d) G. Caliendo, F. Fiorine, P. Grieco, E. Perissutti, V. Santagada, B. Severino, G. Bruni, M.R. Romeo, Synthesis of new 1,2,3-benzotriazin-4-one-arylpiperazine derivatives as 5-HT1A serotonin receptor ligands, Bioorg. Med. Chem. 8 (2000) 533–538;
(e) A.A. Fadda, E. Abdel-Latif, A. Fekri, A.R. Mostafa, Synthesis and docking studies of some 1,2,3-benzotriazin-4-one derivatives as potential anticancer agents, J. Heterocycl. Chem. (2019), https://doi.org/10.1002/jhet.3452.

[17] P. Prakash, B. Aruna, A.A. Sardesai, S.E. Hasnain, Purified recombinant hypothetical protein coded by open reading frame Rv1885c of Mycobacterium tuberculosis exhibits a monofunctional AroQ class of periplasmic chorismate mutase activity, J. Biol. Chem. 280 (2005) 19641–19648.

[18] P.W. Rose, A. Prlić, A. Altunkaya, C. Bi, A.R. Bradley, C.H. Christie, L.D. Costanzo, J.M. Duarte, S. Dutta, Z. Feng, R.K. Green, The RCSB protein data bank: integrative view of protein, gene and 3D structural information, Nucleic Acids Res. 45 (2016) D271–D281.

[19] P. Csizmadia, September. MarvinSketch and MarvinView: molecule applets for the World Wide Web. In Proceedings of ECSOC-3, the third international electronic conference on synthetic organic chemistry, September 1ą30 (1999) (p. 367ą369).

[20] R. Huey, G.M. Morris, AutoDock tools, The Scripps Research Institute, La Jolla, CA, USA, 2003.

[21] O. Trott, A.J. Olson, AutoDock Vina: improving the speed and accuracy of docking with a new scoring function, efficient optimization, and multithreading, J. Comput. Chem. 31 (2010) 455–461.

[22] E.F. Pettersen, T.D. Goddard, C.C. Huang, G.S. Couch, D.M. Greenblatt, E.C. Meng, T.E. Ferrin, UCSF Chimera-a visualization system for exploratory research and analysis, J. Comput. Chem. 25 (2004) 1605–1612.

[23] W.L. DeLano, Pymol: an open-source molecular graphics tool. CCP4 newsletter on protein, Crystallography 40 (2002) 82–92.